EXPERIMENTAL INVESTIGATION OF TRANSIENT ENHANCED DIFFUSION OF PHOSPHORUS IN SILICON IN THE MeV RANGE

By

LAHIR S. ADAM

A THESIS PRESENTED TO THE GRADUATE SCHOOL OF THE UNIVERSITY OF FLORIDA IN PARTIAL FULFILLMENT OF THE REQUIREMENTS FOR THE DEGREE OF MASTER OF SCIENCE

UNIVERSITY OF FLORIDA

1997

To my parents

CHAPTER 1
INTRODUCTION

1.1 Introduction

One of the most important inventions in the field of modern physical sciences is the invention of the transistor by Shockley, Bardeen and Brattain. This invention enabled transistors to replace vacuum tubes which were the most commonly used devices until then. One of the crucial developments in the field of electronics was the invention of the integrated circuit by a team of researchers at Texas Instruments, Incorporated. Until this invention, the manufacture of electronic devices was in the form of discrete devices or individual transistors. This invention showed the world that it was possible to integrate many devices in a single chip and hence get more functionality. This invention happened in the late 1960s. Today, the feature sizes are down to about 0.35 microns, and research is continuing on reducing feature sizes even more. At the present rate of development of the integrated circuit (IC) industry, the feature sizes keep reducing at an average rate of 11% per year. The Pentium Pro

manufactured by Intel Corporation--which is manufactured on 0.35 micron technology - has 21 million transistors in it.

Today we are in the border between Very Large Scale Integration (VLSI) and Ultra Large Scale Integration (ULSI). The development in the semiconductor industry has not only been in terms of the number of devices that can be integrated into a single chip, but also, in the developments that have been made in the field of electronic materials. When Shockley invented his transistor, it was a germanium (Ge) transistor that was crudely made and difficult to control in terms of characteristics due to the small energy gap of Ge (0.66 eV). One of the most ingenious developments in modern times is to make use of silicon (Si) instead of Ge as the starting material for the manufacture of integrated circuits. Of course, the need here is to use high purity silicon. The other main advantage of silicon over other materials is that it has a native oxide, SiO_2, while the others do not. Also silicon has a bandgap of 1.1 eV which is more suitable for semiconductor manufacturing in terms of control of device characteristics. Of course research has been going on for quite some time to engineer compound semiconductors which are multi-element semiconductors like GaAs, InP, etc. One of the advantages with these semiconductors is that one can tailor the bandgap as desired by varying the composition

of the elements involved. The other advantage is due to the fact that some of these can be used for manufacture of photonic devices. In fact, silicon is very inefficient in producing photons (light) due to its being an indirect gap semiconductor. Although compound semiconductors have their advantages over silicon, silicon is still used in 95% of the semiconductor industry. But, one needs to do continuous research to come up with methods to improve the feature dimensions and control the processes involved. For the level of complexity involved in the manufacture of integrated circuits today, one needs to use both experimental and computer analysis to have insight into the physical mechanisms involved and to analyze the effect of a particular process change or modification. This definitely makes the semiconductor industry more viable than otherwise. Thus the concept of a "virtual fab" comes into being.

1.2 An Example of a Basic Complimentary Metal Oxide Semiconductor (CMOS) n-well Process Sequence

A simple approach to n-well CMOS fabrication process is to use a p-substrate as the starting material and to create a n-well within the p-substrate to form p-channel devices. The n-channel devices are formed on the native p-substrate. The fabrication steps are divided into a series of masking steps that perform a specific

function in the processing chain. The following sequence represents a very simple, basic, fabrication sequence.

- The first mask defines the well - in this case the n-well. This is where the p-channel transistors are to be fabricated. Ion implantation or deposition and diffusion are used to fabricate the wells. Implantation is preferred over diffusion because it is possible to form shallower wells compatible with the fine dimension processes. As diffusion occurs laterally also, it tends to limit the feature dimensions that are possible to achieve. Hence, for closely spaced structures a shallow well is required.
- The next mask is called the "active" mask, because it defines where the areas of thin oxides are to be grown to implement gates and allow p-type or n-type source/drain diffusions to be formed. Normally a thin layer of silicon dioxide (SiO_2) is grown and covered with SiN. This is used as a masking layer in the following steps.
- The next step is usually the channel-stop implant. Here the areas that do not have transistors are masked with a photoresist mask and doped so that the doped region, in conjunction with the thick field oxide (grown in the next step) that covers these areas, aids in preventing conduction between unrelated transistor source/drains.

- Following this implant, the photoresist mask is stripped, leaving the active regions. The thick field oxide is grown. This grows in areas where the SiO_2/SiN sandwich is absent. The oxide grows both vertically and laterally under the SiO_2/SiN sandwich. This causes a slight loss of feature dimensionality.
- Next, in most processes, a "threshold voltage adjust" step is performed. This is because usually the polysilicon which is used as the gate is doped n^+. In most processes, for normal doping concentrations, this produces a threshold voltage of ~ 0.5 to 0.7 volts in the n-transistors and ~ -1.5 to -2.0 volts in the p-transistors. So, this means that the threshold voltage of the p-transistors have to be compensated more than their n-doped counterparts. This is done by selectively introducing a negatively charged layer at the silicon/oxide interface. This moves the channel from the silicon/oxide interface deeper into the silicon, creating a "buried channel" device. Following these two steps, the gate oxide is then grown.
- Following this, the surface is covered with polysilicon and etched to get the required pattern. This leads to a "self aligned" gate.
- The n^+ areas of implantation (to dope the source, drain, polysilicon and to form a ohmic contact for the n-well) are then defined and implanted and annealed.

- The complement of the n^+ mask is used to define the p-active areas and the p-implants and anneals are done.
- Contacts are then defined and etched to the silicon surface or to the polysilicon regions.
- Metallization is done with Aluminium (Al), Tungsten (W), Platinum (Pt), etc, and selectively etched to produce circuit interconnections.
- Finally the wafer is passivated to protect the chip from contamination and etched to the contact bond pads for wire bonding.

The above sequence describes the basic steps involved in device fabrication. A complete MOS fabrication sequence involves these steps and many more steps for "fine tuning" that are dependent on the individual processes leading to a total of around 200 steps by the time the finished wafer comes out of the fabrication facility. In addition there are also device characterization techniques that are an integral part of wafer fabrication. In fact one of the device characterization techniques - Secondary Ion Mass Spectroscopy (SIMS) - was used in this study and is explained in detail in the next chapter.

In this study, we concentrate only on the implantation and annealing steps in the fabrication sequence. The reason for this is because these are the main methods for doping a semiconductor and these play a vital role in controlling the electrical characteristics

of a device. Implantation as a technique, is used as a means of introducing controlled amount of dopants into the wafer. This study concentrates on impalnts in the high energy range. High energy implantations are especially used in retrograde well manufacture and for latch-up immunity improvement. Retrograde wells are made through high energy implants as this drives the dopants deeper into the well and so minimizes the lateral spread during subsequent annealing. Further, the retrograde profile also improves the latch-up immunity by increasing the conductivity at the bottom of the well, which decreases well resistance and hence enhances latch up resistance. By employing high energy impants to manufacture retrograde wells, the packing density is improved because of the reduction in p^+ to n^+ spacing. As explained in detail in the next chapter, diffusion is one of the crucial steps in wafer fabrication. Usually it is preceded in the fabrication sequence by ion implantation that creates a lot of defects. Diffusion is "isotropic" in the sense that diffusion takes place both laterally and vertically in the wafer. So, to control the layer dimensions and hence the device performance characteristics, one needs to have as much control and understanding as possible over diffusion. To achieve this end, one of the means of exercising control over diffusion is to use a reduced thermal budget involving low annealing times or low temperatures. During these

processes, due to the very high number of defects generated by ion implantation, the species interact with the defects and until they return to their equilibrium values, enhanced diffusion that is reflected by an enhancement in the diffusivity is seen. Thus, the name transient enhanced diffusion (TED). This effect is crucial as it can alter the junction depths on the order of a few tenths of a micron. In the past, this effect was not of much importance as the device dimensions were much larger. Now-a-days, with ever shrinking feature dimensions, and hence shallower junctions, this effect is becoming ever more important.

This research is to study the effect of high energy implants on transient enhanced diffusion. As stated earlier, diffusion is isotropic and, hence, for better dimension control, implantation is used to introduce dopants into the wafer. Further, through implantation, we can also precisely control the dopant concentration in the regions of the wafer. Nevertheless, a diffusion step is still required to electrically activate the dopants and to drive them to the required depths. This is commonly referred to as annealing. As explained later in this thesis, the two main parameters that affect the enhancement of transient diffusion are the implant dose and the implant energy. High energy implants are becoming increasingly useful today, especially in the manufacture of wells. This is because wells are

typically quite deep and hence need high implant energies to attain the required depth. They are also used to make certain structures like retrograde wells, which are not possible to make at low implant energies.

Before concluding this chapter, it is instructive to note that while it may seem that wafer fabrication is just a sequence of repeating a few basic steps, it has to be appreciated that these steps involve maintaining feature dimensions and expected device performance characteristics of sub - micron technologies with very high precision, reliability and repeatability.

CHAPTER 2

BACKGROUND

2.1 Introduction

This chapter provides the necessary background to understand this study. The theory behind diffusion and implantation will be presented in sections 2.2 and 2.3. This study mainly involves implantation and diffusion. As stated in the previous chapter, implantation and diffusion have a major impact on feature dimension control and electrical characteristics. As feature sizes continue to shrink, the junction depths are becoming more shallow. To fabricate shallow junctions, the thermal budget has to be reduced. But during the time that the species interact with the defects that are generated by implantation, enhanced diffusion is seen. This enhancement becomes more significant in the light of the reducing feature dimension of today. While reviewing diffusion, special emphasis shall be laid on oxidation enhanced diffusion (OED) because OED was the precursor to transient enhanced diffusion (TED) and leads easily to understanding TED. For Boron and

Phosphorus, OED involves injection of interstitials from the silicon-oxide interface into the bulk, while TED involves injection of interstitials from the damage region, deeper into the bulk and towards the surface. OED involves injection of interstitials from a plane, whereas, TED involves injection of interstitials from the whole damage region. A brief review of the literature in the field of transient enhanced diffusion will be presented in Section 2.4. Finally, any process analysis employs characterization techniques. In this study, the characterization technique involed was Secondary Ion Mass Spectroscopy (SIMS) and a theoretical explanation of this technique would be presented in Section 2.5.

2.2. Ion Implantation

Ion implantation is a process by which ions at desired energies are introduced directly into the substrate. The concentration depends on the dose while the depth depends on the implant energy. As a technique, ion implantation is used in VLSI fabrication to add more dopants ions, usually selectively, into the surface of the silicon wafers. This technique is superior to the earlier doping methods because it offers precise control over the dose. This advantage has caused implantation doping to become dominant in a number of process

applications. To achieve this end the species should be implanted in the exact quantity specified, at the energy required to get the required depth and electrically activated when required. It is also instructive to note that all this must be achieved at as small a damage as possible to the silicon lattice structure.

The ion beam current in implanters usually ranges from $10\mu A$ to 30mA, depending on the implant species, energy and model of the implanter. The number of implanted ions per unit area is defined as the dose, ϕ. Typical doses range from 10^{11} - 10^{16} atoms/cm^2. The dose (in atoms/cm^2) is related to the beam current I(in amperes), beam area A (in cm^2) and the implantation duration t(in sec) by:

$$\phi = (I\,t) / (q_i\, A)$$

where q_i is the charge per ion (normally equal to one electronic charge, $1.6 * 10^{-19}$ C).

To control the number of impurities implanted into the substrate, it is necessary to know where the implanted ions are located after implantation. In other words, it must be possible to predict the depth distribution or the profile of the as-implanted atoms. This is necessary to design a new fabrication sequence or to modify an existing one. To achieve this end, it is necessary to make predictions based on theoretical models which are based on the energy interaction mechanisms between the impinging ions and the substrate.

In this regard there are a few definitions that are associated with ion implantation profiles. The total distance that an ion travels before coming to rest is termed the *range*, R. The projection of this range along the implantation direction is called the *projected range*, R_p. As an ion moves, it transfers energy by collisions with the target nuclei (nuclear collisions) and by Coulombic interaction with the electrons (electronic stopping) in the target material until it finally comes to rest.

2.3 Diffusion

To understand the mechanism of diffusion of point defects in silicon, it is important to know the process by which diffusion occurs. The mathematics behind the diffusion phenomena are based on two laws. They are as follows:

Fick's First Law[1]: If there is an impurity concentration gradient present $\delta C/\delta X$, in a finite volume of a substance, then there will be a tendency for the impurity material to move so as to cause a decrease in the gradient . If the flow persists for a sufficiently long time, the material will become homogeneous and the net flow of matter will cease. This material flow is expressed in the one dimensional case, as a flux J, which is given by:

$$J = - D\ (\delta C(x,t)\ /\ \delta X) \qquad (1)$$

where D is the constant of proportionality called the diffusion constant or the diffusivity. The above equation is called Fick's First Law.

Fick's Second Law[1]: Here the case of a finite volume of material in which the impurity gradient decreases with time is considered. In this case, the impurity concentration is also changing with time. Since this is a condition frequently encountered during a diffusion process, Eq. 1 must be modified to include this effect. For example, if we consider a bar of cross - sectional area (fig. 1) with the x-axis along its center, we obtain the following: An element, Δx thick (that is assumed to be very small) along the x-axis has a flux J_1 entering on one side and J_2 leaving on the other. J_1 can be related to J_2 by the expression:

$$J_1 = J_2 - \Delta x\ (\ \delta J/\ \delta X) \qquad (2)$$

Since the amount of material that entered the element in unit time, J_1, is different than that which left J_2, the concentration within the element must change with time, $\delta C/\delta t$ (assuming that no impurity materials are formed or consumed in the matrix). The volume of the element can be expressed as unit area times the thickness, and thus the net increase in matter in the element per unit time is given by:

$$J_2 - J_1 = \Delta x\ (\delta C / \delta t) = -\Delta x\ (\delta J / \delta X) \qquad (3)$$

$$\delta C(x,t)/\delta t = -\delta J/\delta X \qquad (4)$$

Substituting Eq. 1 in Eq.4, Fick's Second law is obtained as:

$$\delta C\ (x,t)/\ \delta t = (\delta/\delta x)\ (D\ \delta C/\delta X)$$

(5)

If the diffusion coefficient is independent of position, as is the case when the dopant concentrations are low, the Eq. 5 reduces to

$$\delta C(x,t)\ /\ \delta t = D\ (\delta^2 C\ /\ \delta X^2) \qquad (6)$$

Eq. 6 is what is commonly referred to as Fick's Second Law.

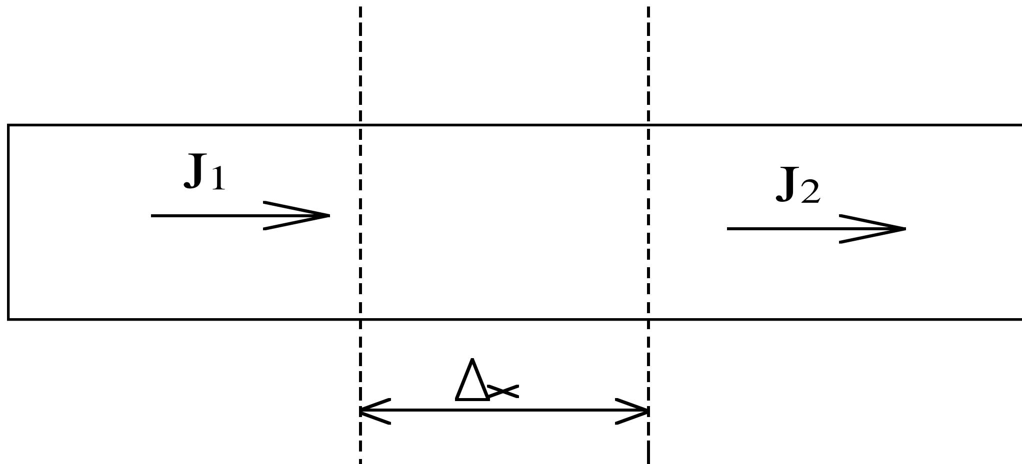

Fig.2.1: Schematic showing an element of volume with flux J_1 entering and J_2 leaving

To get the temperature dependence of the diffusion coefficient, empirical measurements of the diffusion coefficient, D, have shown that

$$D = D_0 \exp\ (-E_a\ /\ kT) \qquad (7)$$

where D_0 and E_a may vary with composition, but are independent of temperature. The temperature T is in °K. This relation is true from thermodynamic theory too. The measured values for activation energy for diffusing atoms in silicon vary from 0.2 - 2eV for the fast diffusing elements (such as He, H_2, O_2, Au, Pt, Na, Ni, etc.,) and to 3 - 4eV for the substitutional impurities (such as B, Ga, P, As and Sb).

The preceding discussion discussed diffusion based on lumped parameters. To understand the phenomena of diffusion we need to consider models on an atomistic scale. A great deal of effort has been expended into identifying these mechanisms.

The presence of an atom at a position other than its substitutional site in a regular silicon cyrstal lattice is referred to as an interstitial. The absence of a silicon atom at its sustitutional site in a regular silicon cyrstal lattice is referred to as a vacancy. Studies[2] have shown that both vacancies and interstitials play a role in the substitutional impurity diffusion in silicon. It has been known that diffusion proceeds by the direct or by the indirect means. Those impurity atoms that do not have a strong bonding interaction with Si atoms are located exclusively at the interstices of the lattice and jump directly between interstices. For example Au^+ is believed to diffuse in this manner.

Certain dopants like Ge[3] and fcc metals[4] are known to diffuse by a vacancy mechanism which need intrinsic point defects as the diffusion source. It has also been proposed by Fair[5] to be the controlling mechanism in Si. Since this study involves Phosphorus, it is instructive to note that Phosphorus diffuses predominantly by an interstitial mechanism.

2.3.1. The Vacancy Model

The vacancy model of Fair[5] is based on the premise that the diffusion coefficient of an impurity is dominated by the interaction of the impurity with vacancies. If the impurity diffusion is dominated by an acceptor type monovacancy mechanism, the diffusion coefficient is approximately proportional to the acceptor monovacancy concentration which is described in the following equations. In the following equations, the notations used are as follows:

D : Diffusivity

C_v : Vacancy concentration

C_v^* : Extrinsic equilibrium vacancy concentration

${}^{int}C_v^*$: Intrinsic Equilibrium vacancy concentration

V^0 : Neutally cahrged Vacancy

V^- : Single negatively charged vacancy

E_F : Energy of the Fermi level

E_{V^-} : Energy of the single negatively charged vacancy level

E_i : Energy of the intrinsic level

E_C : Energy level of the conduction band

k : Boltzman's constant

T : Temperature in ^{0}K

$$D \; \alpha \; C_v \qquad (8)$$

Assuming equilibrium,

$$C_v = C_v^* \qquad (9)$$

Since monovacancy mechanism alone is assumed to be the cause of diffusion and from basic Maxwell Boltzman statistics,

$$V^0 + e^- \Leftrightarrow V^- \qquad (10)$$

$$C_v^* \; \alpha \; \exp \{-(E_F - E_{V^-})/kT\} \qquad (11)$$

$$^{int}C_v^* \; \alpha \; \exp \{-(E_i - E_{V^-})/kT\} \qquad (12)$$

$$n \; \alpha \; \exp \{-(E_F - E_C)/kT\} \qquad (13)$$

$$n_i \; \alpha \; \exp \{-(E_i - E_C)/kT\} \qquad (14)$$

Therefore,

$$(C_v^*/^{int}C_v^*) = (n/n_i) = \exp \{-(E_F - E_i)/kT\} \qquad (15)$$

So,

$$C_v^* = {}^{int}C_v^* \; (n/n_i) \qquad (16)$$

$$D \; \alpha \; (n/n_i) \qquad (17)$$

Hence,

$$(D/D_i) = (n/n_i) \qquad (18)$$

Since the defects, however, can have various charge states, Eq.8 can be generalized to include all combinations of point defect interactions[6] and is given by:

$$D = D_{Si}^{x} + \Sigma (D^{-r}) [n/n_i]^r + \Sigma (D^{+r}) [n_i/n]^r \quad (19)$$

where D^x, refers to the diffusion coefficient associated with neutral defects, and D^{-r} and D^{+r} refer to the intrinsic diffusion coefficients associated with the charge state, r, of the defect (r=1,2,3,...,m).

2.3.2. The Interstitial - Vacancy Model

A couple of areas of study have shown that apart from silicon vacancies, silicon interstitials also play a role in controlling the diffusion process. These studies have helped us clarify our understanding of diffusion phenomena in terms of the nature of point defects and diffusion processes in silicon. These results have been obtained by the following studies:

- from the studies on the effect of oxidation on stacking fault growth kinetics and diffusion and
- from the analysis of Au diffusion in dislocation free Si.

The stacking fault studies showed that interstitials and vacancies coexist in silicon at high temperatures, under thermal equilibrium, and also under oxidizing conditions. The Au diffusion studies showed that interstitials play a role, and it is possible for

both interstitials and vacancies to coexist. Tan and Gosele[7] have given a detailed analysis on the estimation of the interstitial and vacancy component of self-diffusion in Si based on oxidation enhanced diffusion and oxidation retarded diffusion of dopants in Si.

From a study of Au diffusion in dislocation- free Si, it is found that they can be incorporated as either substitutional impurities Au_s, or as interstitial impurities Au_i. The incorporation as Au_s occurs by the Frank - Turnbull mechanism while the incorporation as Au_i occurs by the kick - out mechanism. In both these mechanisms, the transport of Au atoms occurs via the migration of Au_i, which may jump from one interstitial site to another, or from an interstitial site to a lattice position, to become Au_s.

In the Frank - Turnbull mechanism the interchange involves vacancies in equilibrium and the equilibrium is given by:

$$Au_i + V \Leftrightarrow Au_s \qquad (20)$$

where V refers to the vacancy.

In the kick-out mechanism, the interchange involves interstitials and the equilibrium between the two types of Au sites is given by:

$$Au_i \Leftrightarrow Au_s + I \qquad (21)$$

where I refers to the self interstitial.

Care has to be taken in interpreting these equilibrium conditions. If Eq.10 is controlling, it

means that vacancies are involved in Si self-diffusion, but there is no implication regarding the contribution of interstitials. If Eq.11 is controlling, it means that interstitials are involved in silicon self-diffusion, but this again does not imply that vacancies are also not contributing. The diffusion profile shows an erfc (error function complementary) dependence when only vacancies are involved in the diffusion process and interstitials do not play a role. This implies that the diffusion coefficient of gold is independent of concentration.

At this point it is also worthwhile to mention certain anomalous diffusion effects in silicon though there are other anomalous diffusion effects that are not central to the understanding of this study. One among these is the diffusion that occurs under an oxidizing ambient. As stated earlier the study of oxidation under an oxidizing ambient is the precursor to transient enhanced diffusion (TED) and its study leads quite easily into understanding transient enhanced diffusion.

2.3.3. Diffusion under an Oxidizing Ambient

Hu[8] has proposed that both vacancies and interstitials coexist as intrinsic point defects in silicon and play an equally important role. He also proposed that the diffusion of substitutional impurities in silicon occurs through a dual vacancy - interstitial mechanism. He also stated that the contribution of the

interstitial mechanism as a fraction of the total diffusivity varies with the impurity species. For example, in Boron it is around 0.8 and for Phosphorus it is close to 1. He arrived at this conclusion from an analysis of enhanced diffusion of certain impurities and the formation of stacking faults during thermal oxidation of silicon and analyzing their common features like the crystal orientation and oxidizing ambients. The other important proposition was that thermal oxidation is a surface process that generates excess silicon interstitials. This proposition was essential to explain observation of oxidation enhanced diffusion (OED) in some species and oxidation retarded diffusion (ORD) in others.

Studies[9-16] have observed that, in oxidizing ambients, the diffusion rate varies with the orientation of the crystal lattice. The diffusion rate varies in increasing order as follows: {100} > {110} > {111}. This was because of oxidation enhanced diffusion (OED), an effect that varies with surface orientation. Also, the diffusion enhancement is more under wet oxidation than under dry oxidation. Another phenomenon that has been shown by some authors[17-21] is that thermal oxidation of silicon leads to the formation of oxidation stacking faults (OSF). The growth rate is also dependent on the crystallographic orientation in the order as {100} > {110} > {111}. The growth rate for this phenomenon too

is more for wet oxidation than for dry oxidation . Connecting OED to OSF, leads us to understanding the nature of diffusion in silicon. TEM studies[22,23] have shown that OSF in silicon is of the interstitial type.

The other phenomenon that leads us to believe that OSF growth is due to interstitials is the precipitation of oxygen in silicon. When interstitially dissolved oxygen atoms agglomerate into a SiO_2 precipitate, then a unit volume of silicon is converted into 2.25 unit volumes[2] of SiO_2 incurring a large strain energy. One way to reduce the strain energy due to localized expansion is to provide the necessary volume by emission of self - interstitials or absorption of vacancies. This means that there will be a supersaturation of interstitials or undersaturation of vacancies. The supersaturation of interstitials due to oxygen precipitation has been shown by Hu[24] and Rogers *et al.*[25] to feed the growth of pre-existing OSF.

There was another observation by Mizuo and Higuchi[26] and Antoniadis and Moskowitz[27] that diffusion of antimony is retarded under oxidizing conditions. This is termed oxidation retarded diffusion (ORD). So, this means that antimony diffusion in silicon is mediated predominantly by the vacancies. Hu[2] has also argued this effect in terms of the elastic interaction between a point defect and substitutional atom being dominated by the mismatch in the lattice sizes between them. He says that a larger

substitutional atom is attracted to the vacancy while a smaller atom is attracted to a self - interstitial.

A complimentary phenomenon was observed in studies[28-32] involving thermal nitridation of silicon where the opposite effects are observed. The diffusion of phosphorus is retarded while the diffusion of antimony is enhanced. So, nitridation generates excess vacancies.

Hence, to point out the salient features of this discussion on OED, the formation of OSF indicates that there is a supersaturation of interstitials and an undersaturation of vacancies during thermal oxidation. This effect is manifested by the diffusion enhancement observed in boron and phosphorus and the diffusion retardation observed in antimony. The fact that OED occurs for antimony under thermal nitridation indicates that nitridation generates excess vacancies. So, from the observation that phosphorus diffusion is retarded under thermal nitridation, we can conclude that the vehicle of phosphorus diffusion is predominantly the self-interstitial, whose concentration is reduced by annihilation with the excess vacancies generated during thermal nitridation.

2.4 Brief Literature Survey of Transient Enhanced Diffusion

Since phosphorus diffuses predominantly by an interstitial mechanism[33,34], it is of interest to quote a few references on the properties of interstitials.

One of the first papers to suggest that gold diffuses by an interstitial mechanism and thus enable one of the means of study of the silicon interstitials was the paper by Gosele, *et al*[35],. which showed that the vacancy or the Frank - Turnbull mechanism cannot account for the fact that Au diffuses in Si as $C_s^m \alpha \sqrt{t}$ as suggested in the literature. But, they were able to account for this relationship through the interstitial mechanism.

Bronner and Plummer[36] have proposed that high concentration phosphorus diffusion, argon - ion implantation and mechanical damage of a silicon surface all act as sources of interstitials. They proposed this theory based on gettering experiments. In their experiment, the front and back of the wafers were implanted with gold and annealed for three hours in a nitrogen ambient. These samples were chemically etched to remove any surface gold pile up. In some of their samples, the back of their wafers were implanted with argon at 10^{15} atoms/cm^2 at an energy of 500KeV. This was followed by gettering in a nitrogen ambient for 30min. at temperatures varied from 600 - 1000°C. The other samples were damaged with a rotating wheel for about 10μm deep. These were then gettered in a nitrogen

ambient. Bronner and Plummer observed that more gold is gettered at the back than at the front. They reasoned that this was because the backsurface gettering region changes the point defect equilibria near the back so that more gold is interstitial and so diffuse faster. Zimmerman and Ryssel[37,38], have also conducted experiments that are in tandem with the findings of Bronner and Plummer.

Coffa, *et al.*[39], have proposed that the kinetics of the gettering process of Pt in Si is driven by the dissolution of immobile substitutional Pt atoms into interstitial sites that is helped by the Si self - interstitials themselves. They have calculated an activation energy of 0.4 eV.

Now that some of the literature behind the properties of Si interstitials have been presented, albeit very briefly, a brief survey of the previous experiments linked to transient enhanced diffusion of dopants would be presented.

For around the past fifteen years, various authors[40-55] have reported anomalous dopant diffusion behavior in their experiments. One of the experiments performed by Hodgson *et al*[40]. reported enhanced Boron diffusion in the tail region that was independent of anneal temperature, when they annealed implanted Boron at temperatures ranging from 900°C - 1250°C. While analyzing the above mentioned results, Hodgeson *et al.*[40]

assumed that the atoms in the tail of the Boron profile consisted mostly of channeled atoms. Channeled atoms have a high probability of coming to rest on an interstitial site. The transient diffusion was explained by a fast initial diffusion of the interstitial atoms until they are trapped to recombine with a vacancy. Once the excess interstitials are removed in this manner, only normal Boron diffusion occurs. Hopkins *et al.*[41], used many anneals and etches to strengthen this position. In their experiment Boron was implanted into Si. Then, some of the samples were etched so as to remove the high damage area leaving only the implant tail. After their anneals, they found that all the samples irrespective of whether they were etched or not, showed the same enhanced tail diffusion when they analyzed the slopes of the annealed tail profiles. Thus, they concluded that damage did not play a large role in the transient diffusion effect.

But, interestingly, there was another experiment conducted by Cho *et al.*[42], that reported another conclusion that was contrary to that presented by Hopkins *et al*[41]. In the experiment of Cho *et al.*[42], they analyzed transient enhanced diffusion through multiple implants of ^{10}B and ^{11}B. They first implanted ^{11}B and then annealed those samples for times greater than the length of the transient diffusion. Then they implanted those samples with ^{10}B. If the ^{11}B profile showed any transient

effect, then this could be concluded as due to the damage. If, on the other hand, there was no transient diffusion seen, then one could attribute it to the interstitial Boron in the tail of the profile. They showed that there was a transient diffusion of the ^{11}B profile and thus concluded that implant damage did play a role in transient enhanced diffusion.

In another experiment to determine the depth dependence of transient enhanced diffusion, Servidori *et al.*[47], did a series of experiments in which they changed the depth of the damage and dopant profiles independent of each other. Shallow and deep dopant profiles of B, P, As, Sb were created through a series of predepositions and anneal steps. Then ^{28}Si implants were used to create shallow and deep damage profiles for each of the doping conditions. The implant conditions were such that both the shallow and the deep damage profiles created an amorphous region at the surface. These samples were then annealed at 700°C to 900°C and analyzed the resulting profile. They reported that the shallow region showed retarded diffusion while the deep profile showed enhanced diffusion. They correlated these results with strain profiles obtained from X-Ray diffraction measurements. These strain profiles showed a shallow region with negative strain and a deep region with positive strain. They theorized that the region of negative strain was rich in vacancies, while the region

of positive strain was rich in interstitials. Since it is well known that Boron diffuses predominantly by an interstitial mechanism, the implantation creates a near surface region rich in vacancies with the deeper region being rich in interstitials. This was one of the first experiments to show that implantation creates vacancy excess in the near surface region with a vacancy rich region deeper in the substrate. But, it should also be noted that they were not able to show similar results in their Phosphorus samples even though Phosphorus too diffuses almost completely through an interstitial mechanism.

Michael *et al*[48]., studied the effects of anneal times and temperatures on the transient enhanced diffusion of Boron. The annealed their implanted samples at temperatures between 800°C - 1000°C. They determined that the decay times were approximately 45 min at 800°C and in the order of a second at 1000°C. As the temperatures were decreased, less transient diffusion was observed. They argued that this was because of the recombination rate of excess defects being lower at lower temperatures. But, it should also be pointed out that their peak Boron concentrations were extrinsic at the anneal temperatures used. Since extrinsic diffusion has certain anomalous effects of its own, interpretation of the above effects tend to become difficult.

One of the early experiments to determine the time dependence of the transient diffusion was conducted by Miyake *et al.*[50]. They implanted Boron and annealed for various times for temperatures ranging from 800°C to 1000°C. using a Gaussian approximation, the diffusion coefficient was calculated as a function of time. Boron diffusion was modeled as follows:

$$D(t) = D_i + D_0 \exp(-t/\tau)$$

where D_i is the intrinsic diffusivity, D_0 is the enhanced Boron diffusivity at time t= 0 and τ is the time constant for the transient diffusivity. Using this scheme they fit their experimental data and calculated activation energies of -1.1eV for D_o and 1.6eV for τ. By relating these values to the formation energy of vacancies and the migration energies of the boron - vacancy pairs, they conclude that the point defect causing the transient Boron diffusion is the vacancy. But, this argument relies heavily on the premise that intrinsic Boron diffusion is caused mainly by a vacancy mechanism. This is contrary to most of the experimental results to date.

In the experiments by Sedgwick *et al.*[51], the effects of surface amorphization on the transient diffusion was observed. They implanted Boron at high doses into both crystalline and amorphous silicon. In the case of the amorphized samples, no transient diffusion was observed. They explained this as follows: In the case of

crystalline samples, a very high concentration of point defects was generated. Until these defect concentrations returned to their equilibrium values, enhanced Boron diffusion can be seen. But in the case of the amorphous samples, the amorphous region very quickly regrows - typically in the order of a few milliseconds - into a single crystal, eliminating all the point defects that were created by the implant. Thus no transient diffusion was observed. The interstitials generated by the implant beyond the amorphous - crystalline interface are not able to come up to the surface due to dislocation loops being present at the boundary. These dislocation loops act as sinks of the point defects. The other observation - that could not be explained - that was made by the authors of this paper was that at high Boron concentrations, Boron appeared to precipitate in the amorphous samples but not in the crystalline samples.

Packan and Plummer[55], have studied the effects of transient diffusion of low concentration Boron in Si due to ^{29}Si implantation damage. They used low doses of 1 * 10^{12} ions/cm^2 to 1 * 10^{14} ions/cm^2 and low energies of 160KeV. They observed that the transient movement is the largest for the highest dose and the lowest anneal temperature. They also observed that doubling the implant dose did not double the diffusion coefficient. The authors acknowledged that they could not propose a mechanism to explain this observation at that time.

Giles[56], investigated the transient enhanced diffusion of phosphorus in silicon at doses and energies below the amorphization threshold and has shown that the transient diffusion occurs in both the conventional and RTA furnaces. Further, he has also shown that the junction depth increases by 0.1 - 0.2 μm over the conventional diffusion models. He has also proposed a quantitative model of damage annealing that describes the point defect enhancement of dopant diffusion.

Eaglesham *et al.*[57], have reported that the source of the interstitials that cause the transient diffusion in Boron and Phosphorus are the {311} defects only. These defects are rodlike in structure which run along the <110> directions. But it has to be noted that though their experiments were of a similar dose as used in this study ($5 * 10^{13}$ ions / cm^2), their implant energies (40KeV) were much below than that used in this study. So their data cannot be extrapolated per se into the regime of the high energy (1 MeV) as used in this study.

Poate *et al.*[58], have proposed a model for transient enhanced diffusion. They state like in the previous reference that the <311> defects are the source of interstitials. They also have developed a "+1.4" model which means that there are 1.4 interstitials created for every ion implanted. This agrees very well with the canonical "+1" model that has been in vogue for quite sometime now.

Cheng *et al.*[59], have identified that extended defects are induced in Silicon by high energy implantations. They used Phosphorus implants of 1.5 MeV and 2.6 MeV and investigated the defects formed by plan view and cross - sectional TEM and found them to be threading dislocations that were inclined dislocations - some of which grew all the way to the surface. They also made a comparison between the difference in dislocation density in the Czochralski samples and the epi - grown samples and attributed these to be due to the strong pinning effect of Oxygen atoms immobilizing the dislocations in the Czochralski substrates.

Rafferty *et al.*[60], studied the transient enhanced diffusion at high energies. In their experiment, they used a Boron marker implanted and annealed to remove its self - TED. Then Si atoms were implanted at energies from 40 KeV to 500 KeV. They then annealed the samples at 800°C and studied the boron depth distribution profiles using SIMS. They observed that the amount of broadening does not increase in proportion to the implant energy. The other interesting note about this paper was that they correlated these results to actual device characteristics.

Most authors believe that the transient diffusion effects observed during post implant are a result of the damage created by the implant. For lower doses, the damage is in the form of point defects, while for the

high dose implants, extended defects are also created. If the dose is sufficiently high, amorphization occurs. It is the interactions of the point defects, extended defects and the amorphized regions that determine the concentrations of the point defects during the high temperature anneals. The interaction of the dopant atoms with these point defects cause transient enhanced diffusion.

High dose implants raise a number of important issues. First, they create extended defects like dislocation loops and stacking faults. These extended defects interact and drastically affect the concentrations of interstitials and vacancies and give rise to different diffusion rates in different regions of the profile[49,51]. Next, they can also create amorphous regions in the sample. These amorphous regions regrow in a matter of a few milliseconds affecting the concentrations of the point defects drastically.

2.5 Secondary Ion Mass Spectroscopy (SIMS)

SIMS technique is one of the Ion beam techniques for compositional analysis. Ion beam bombardment is significantly different from bombardment with electrons. In contrast to electrons/x-ray based techniques which rely only on the electronic structures of each element for identification, ion beam techniques identify the

constitutional elements through their atomic mass values. Some of the ion beam techniques are SIMS, Rutherford Backscattering (RBS), Laser Ion Mass Spectroscpy, etc,. Since only the SIMS technique was used for compositional analysis in this study, this technique alone would be discussed here.

In the SIMS technique, the energetic bombardment of the material with energies from 1 - 20KeV cause collisions with the surface leading to ejection (sputtering) of the material. Due to the energy transfer involved, a small number of atoms that are ejected leave as positively or negatively charged ions. These sputtered or ejected ions are collected by a mass spectrometer for mass to charge separation and detection. The number of ions collected can be counted digitally to produce quantitative data on the concentration and the composition. In fact, this technique is mainly used to get the concentration of the impurity ions as a function of depth - or in other words termed as the depth "profile". This is a destructive technique unlike certain others like Auger Electron Spectroscopy(AES) which analyzes the atomic layers closest to the surface without substantial layer removal.

In order to maximize sensitivity, oxygen atoms are used for sputtering and exciting the electropositive elements like Na, Al, etc., while Cesium (Cs) atoms are

used to produce electronegative elements like P, As, etc,. The beam choice is quite important. With Cesium it is around 0.1ppma. The sputtering process continuously removes the surface atoms. Hence the shallow analytical depth region is advanced further into the sample as a function of time. Usually the ion beam is focussed over a small area of the surface to create a crater with an almost flat bottom. Mass separation analysis is performed only on those ions that are sputtered from the center of the crater.

SIMS has many unique capabilities that make it highly useful for VLSI characterization. The following are some of the capabilities that make it highly suitable for VLSI applications:

- It is capable of detecting all the elements present in the sample
- It can identify elements present in extremely low concentrations as is commonly encountered in semiconductor devices
- It is especially sensitive to elements with very low ionization potentials like Na, K.

The above reasons make it clear as to why SIMS is the most preferred technique when it comes to compositional characterization.

But like all other techniques SIMS has its drawbacks. One has to be aware of its drawbacks to

exploit its advantages to the maximum possible limit. Some of its drawbacks are as follows:

- First the width of the beam decides the sensitivity. Usually the beam widths are 1.0 - 200μ in diameter. The maximum sensitivity is achieved with a wider beam. This is because when the beam is focussed onto a smaller spot, the number of atoms sputtered also correspondingly reduces, leading to reduced sensitivity. It is true that this technique is limited in sensitivity when analyzing very small regions on VLSI devices.
- SIMS suffers from the problem of secondary mass interference. For example, if the sample contains two species of comparable masses, then it becomes difficult to distinguish them using SIMS.
- SIMS is locally destructive.

Apart from the fact that it is a destructive technique, one of the ways to overcome these drawbacks is to use higher system vacuums, higher resolution detectors. But of course these would result in higher cost to the analysis.

CHAPTER 3
EXPERIMENTAL RESULTS

3.1 Introduction

Transient Enhanced Diffusion (TED) has been the primary modeling challenge of the process simulation community. As was seen in the last chapter, implantation is a precise technique for incorporation of dopants in

the wafers. For low implant doses, most of the damage results in the generation of point defects. However, as the dose is increased, these point defects interact with each other leading to formation of extended defects. At high enough implant doses, the number of point defects created is so high that the lattice is no longer crystalline and becomes amorphous. For Phosphorus implant, this occurs around a dose of $2*10^{14}$ atoms/cm^2. By annealing at high temperature, most of the implant damage can be repaired. Both point defects and extended defects can be removed by these anneals. During these anneals, the interstitials and vacancies recombine with each other or diffuse to the surface which serves as recombination sites. However, until the defect concentrations return to their equilibrium values, anomalous dopant diffusion can occur which is manifested by an increase in the diffusivity constant from their equilibrium values.

This work is relevant because as stated in Chapter 1, MeV implantations are increasingly used in semiconductor manufacturing - especially in well manufacture technology. Section 3.2 shall give a description of the experimental setup. First a flow chart shall be presented followed by a detailed description of the experiment. The raw data shall be presented in Section 3.3. Section 3.4 presents and discusses the plots of the diffusivity enhancement at

the doses and temperatures used in this study. Finally Section 3.5 contains a discussion on the implications of the results presented.

As stated in Section 2.4 in the last chapter, high dose implants present the problem of formation of extended defects like dislocation loops and stacking faults. These defects interact changing the point defect concentrations drastically. Further, there is also the problem of crystal amorphization and regrowth. Under high doping cases, the doping may also be extrinsic at the anneal temperatures used leading to anomalous diffusion effects. To resolve these problems, it was decided to concentrate on two doses. A dose of $5*10^{13}$ was chosen so as not to expect amorphization while another dose of $2*10^{14}$ was chosen so as to be around the amorphization threshold. Of course, the main theme of this study was to analyze the effects high implant energies had on the transient diffusion of dopants. The species used in this study was Phosphorus.

3.2 Description of Experiment

The following figure represents a flow chart of the experiment done in this study.

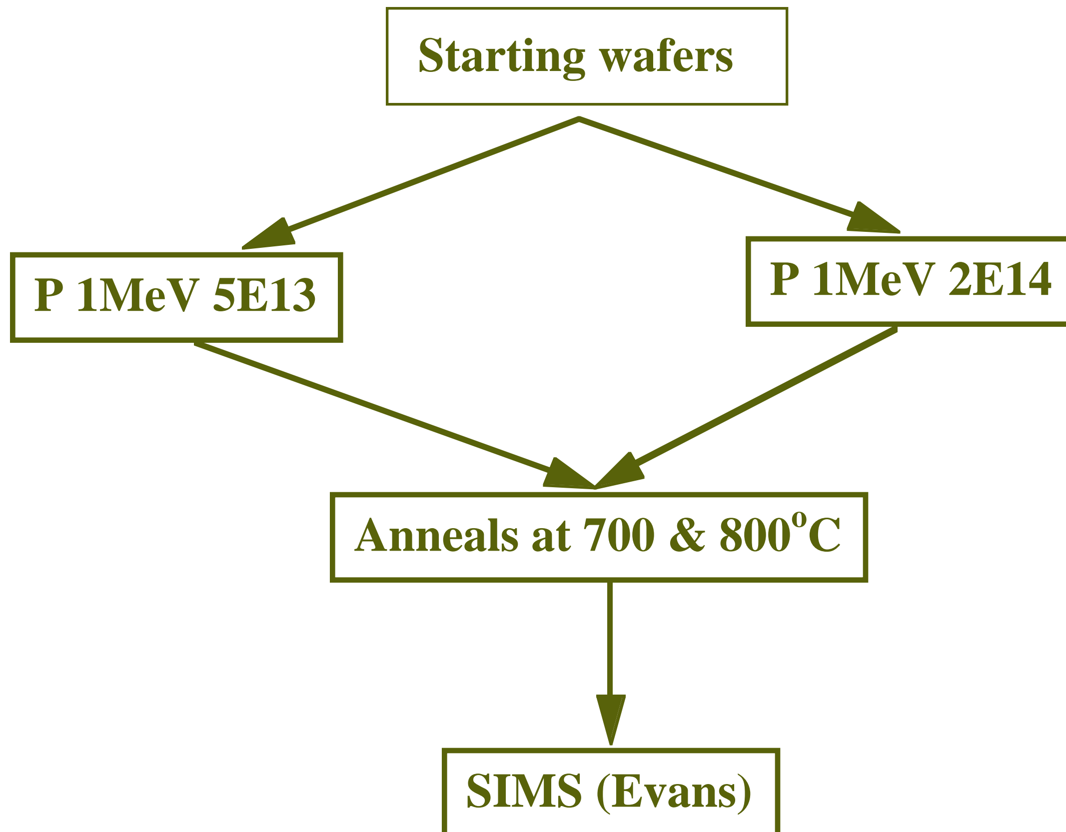

Figure 3.1: Flow chart describing the flow of the experimental set up

The wafers used in this study had a crystalline orientation of <100>. They were grown by the Czochralski method. There are different methods by which the wafers could be grown. The main methods of growth are:

(I) Czochralski method of growth (CZ)

(II) Float Zone growth technique (FZ)

The main difference between the CZ and the FZ methods of growth is that the CZ wafers have a higher concentration of Oxygen atoms since they are grown from a silica crucible. The typical concentrations are in the order of 10^{18} oxygen atoms/cc. Since CZ wafers are used

predominantly in the industry, they were used in this study also.

The diameter of the wafers was eight inches. These wafers were implanted with 0° tilt with Phosphorus at the doses of $5 * 10^{13}$ and $2 * 10^{14}$ ions/cm^2 and an energy of 1MeV (Million elctron volts). The implants were done at Eaton Corporation. After dicing, the wafers were annealed at 700°C and 800°C at various times. The annealing times at 700°C were 20 minutes, 40 minutes, 1 hour, 2 hours, 4 hours and 6 hours. For the anneals at 800°C the annealing times were 15 minutes, 30 minutes, 60 minutes, 90 minutes and 2 hours. These times were selected based on what was to be expected from a study of low energy implants. The furnace used was a conventional furnace. After the desired temperature was reached, the wafers were loaded onto the center zone of the furnace. Fast push and pulls were used. The ambient under which the experiments were done was Forming gas (90% N_2 and 10% H_2). Care was taken to see that the furnace was calibrated and that the flow and the temperatures remained steady at the desired values for the duration of the time of the experiments.

After the samples were successfully annealed, they were sent for Secondary Ion Mass Spectroscopy (SIMS) analysis to Evans East Corporation who are specialists in materials characterization. The SIMS profiles of these samples were then taken and fit to simulated

profiles. The simulator used for this purpose was the Florida Object Oriented FLOOPS Simulator (FLOOPS). Diffusivity enhancement data was extracted from the simulated and experimental profiles and the data analyzed as described in the next chapter.

3.3 Raw Data

The figures 3.2 (a)-3.2 (l) represent the raw data i.e., the profiles at the conditions as indicated on the figures. The profile after annealing at the shortest times show very marginal enhancement as expected. We also note that the profile has not moved much within the temperatures and the times for which the experiment was done.

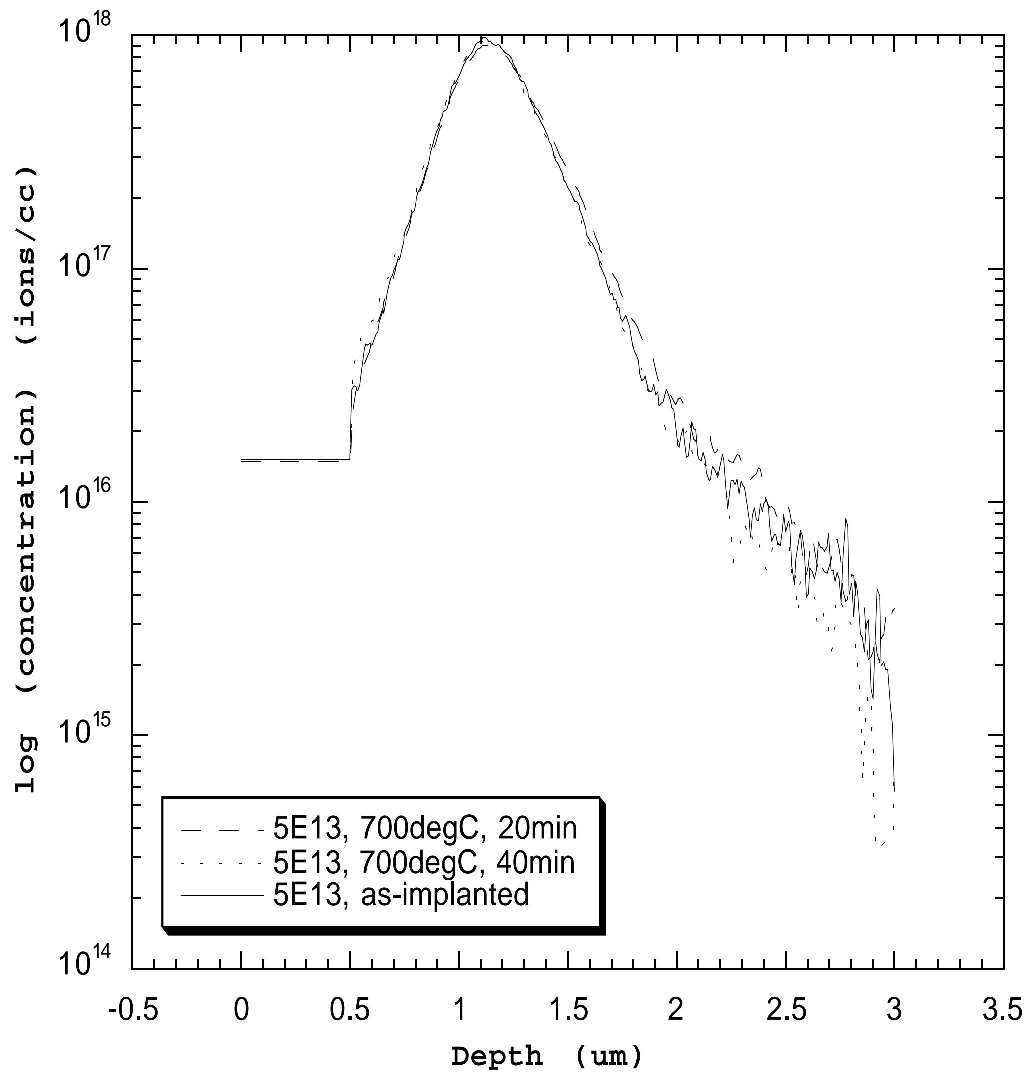

(a)

Figure 3.2: Concentration profiles

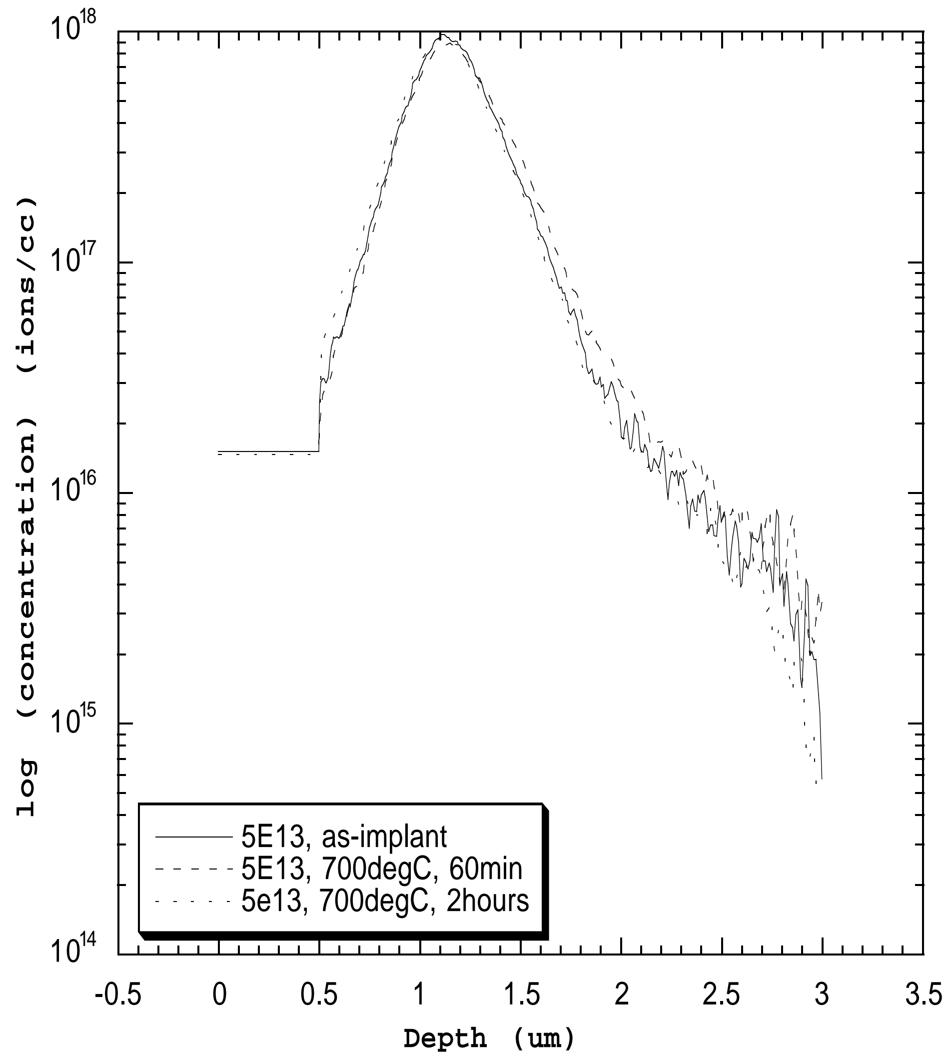

(b)

Figure 3.2 continued

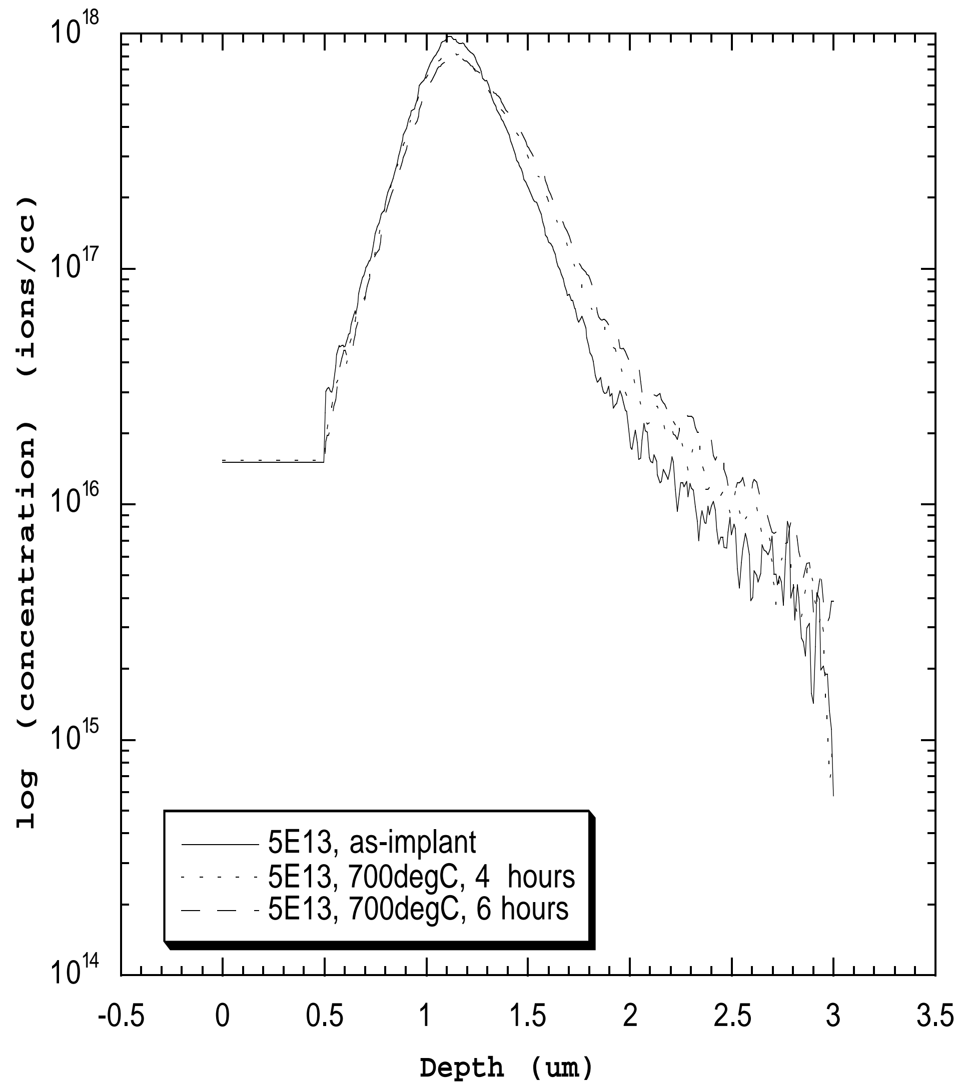

(c)

Figure 3.2 continued

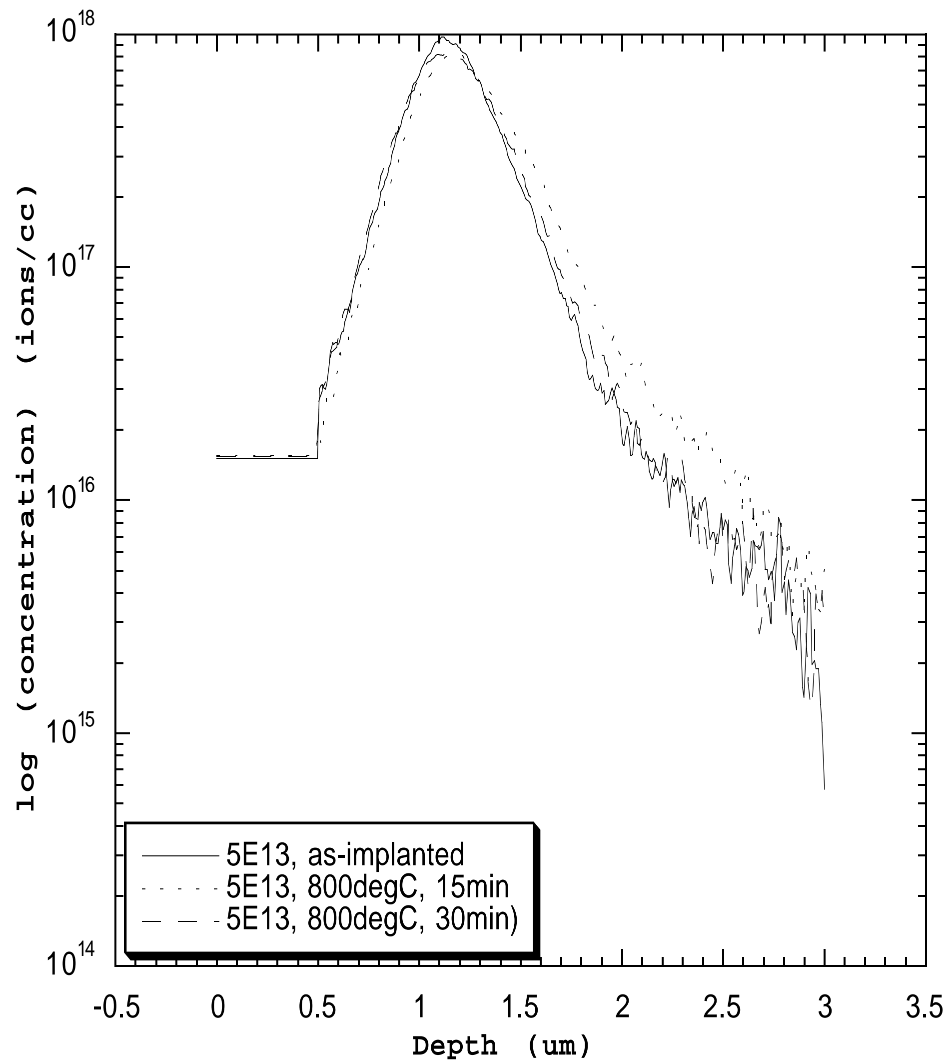

(d)

Figure 3.2 continued

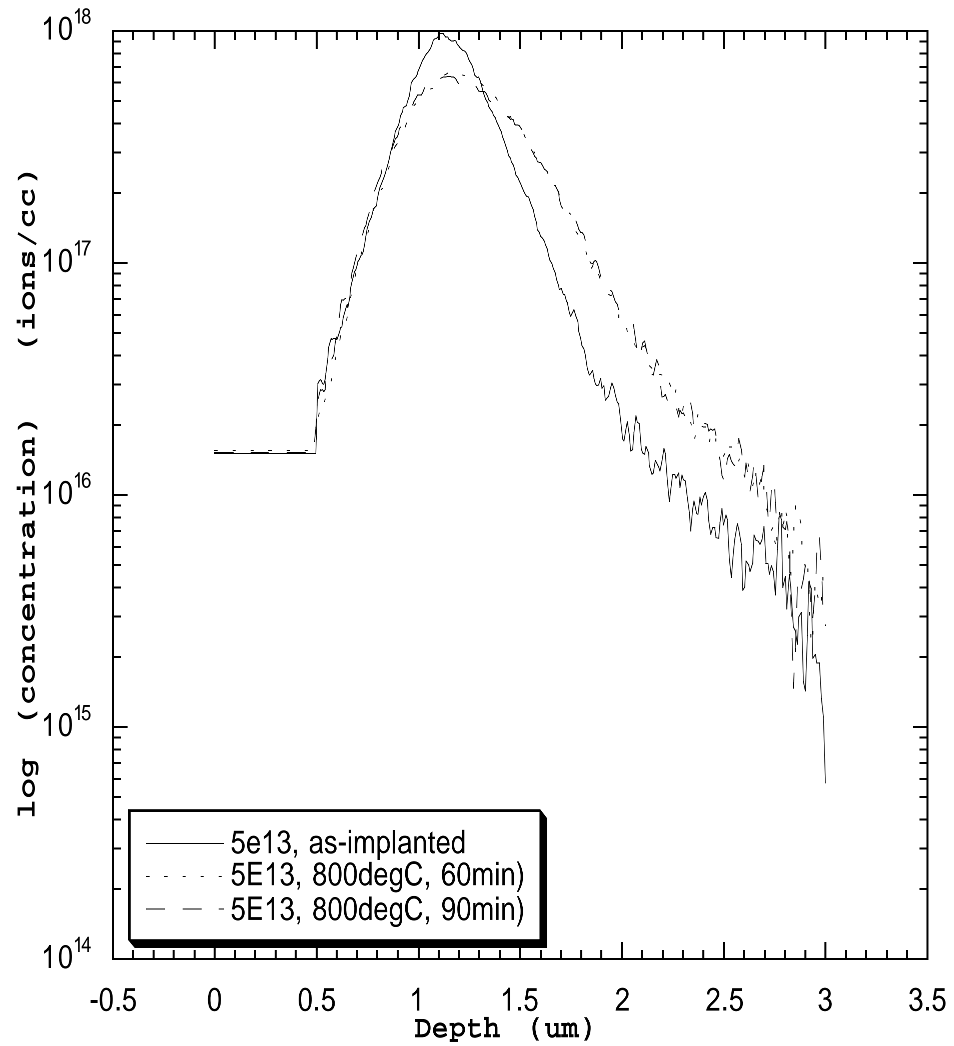

(e)

Figure 3.2 continued

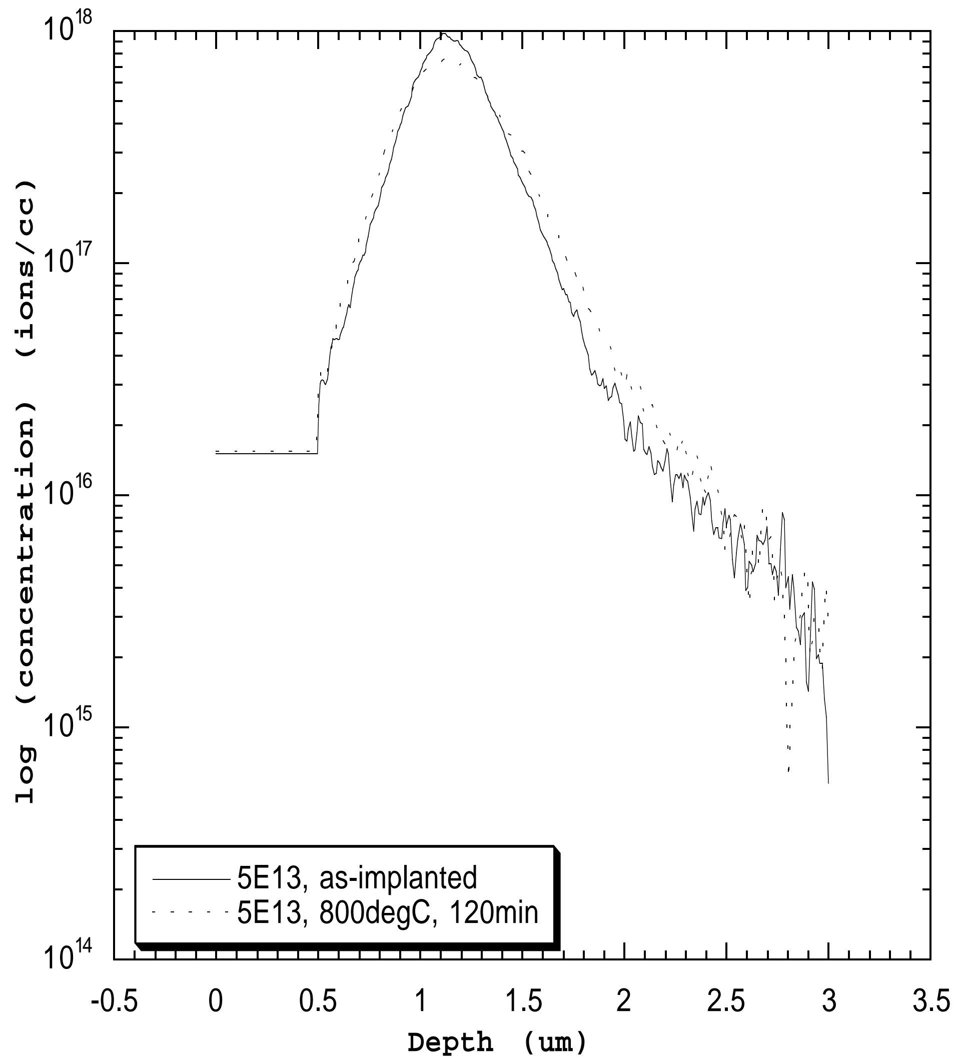

(f)

Figure 3.2 continued

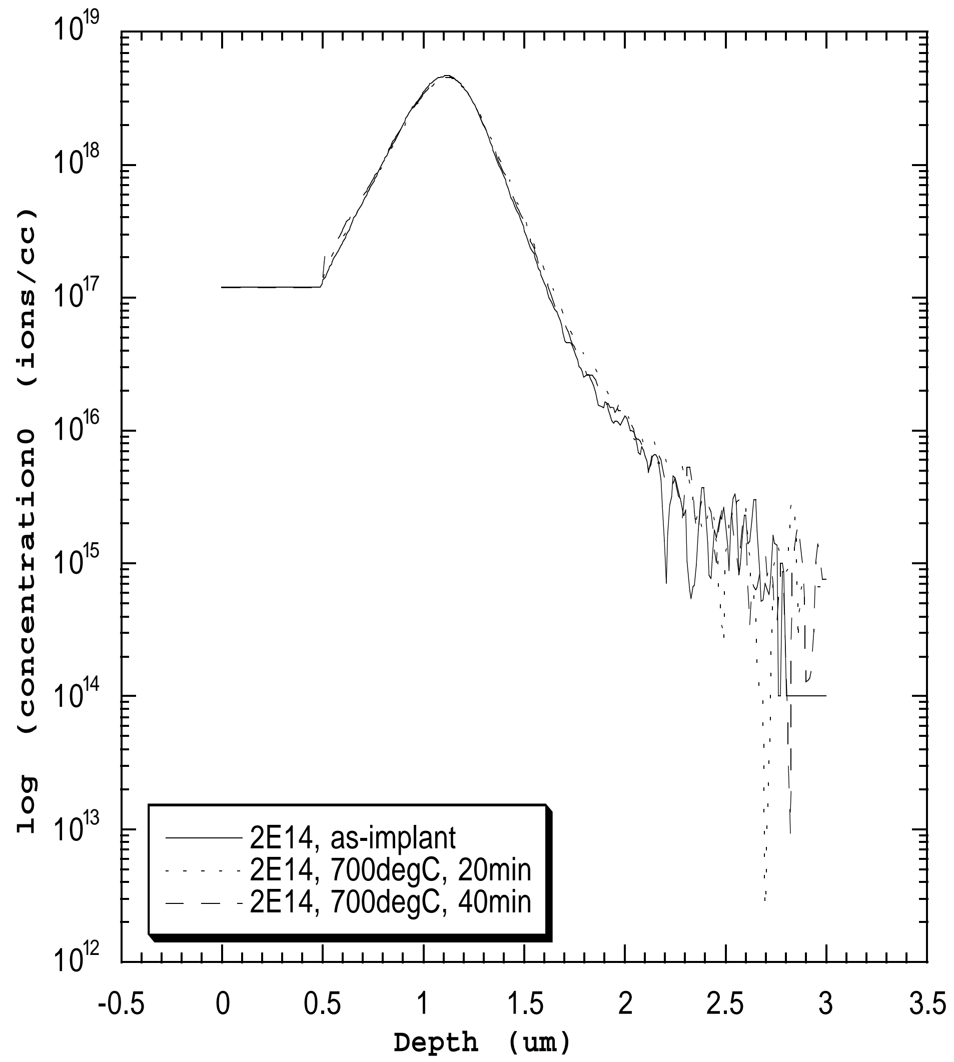

(g)

Figure 3.2 continued

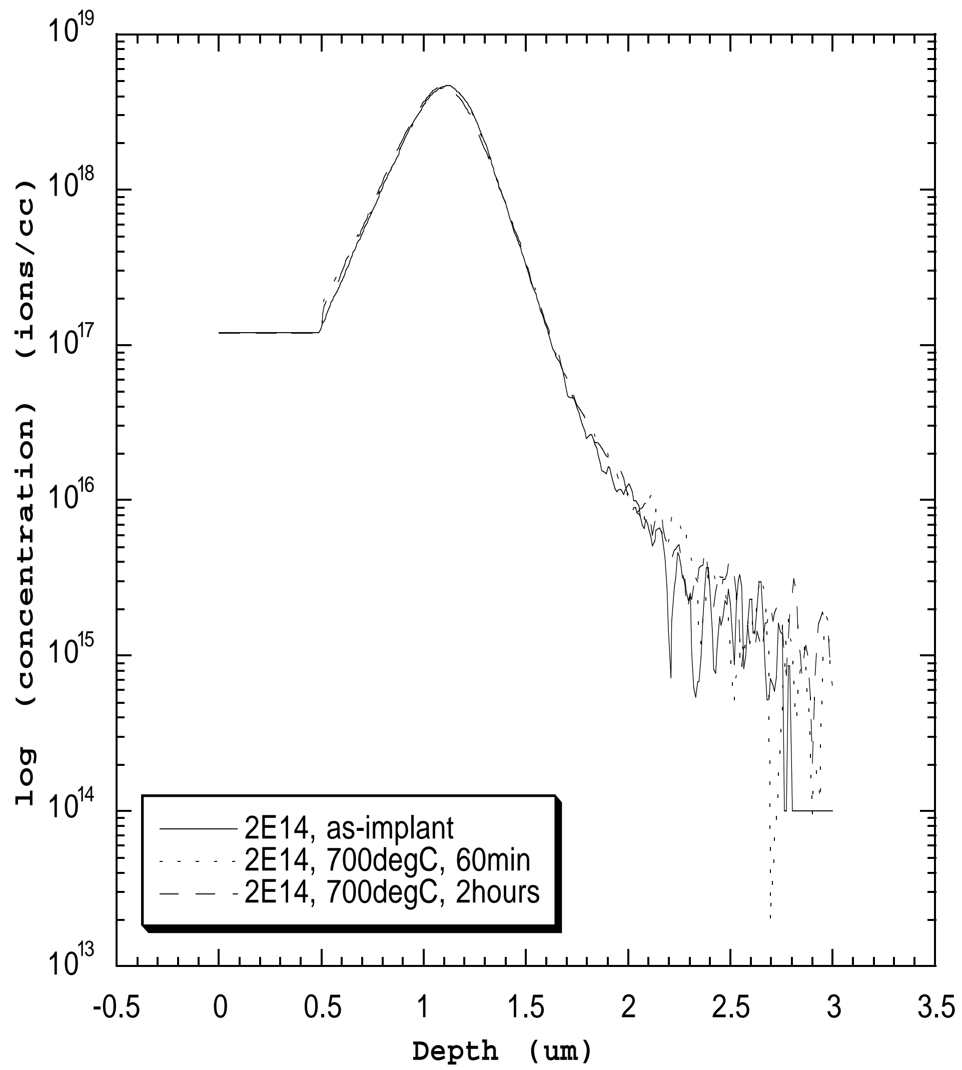

(h)

Figure 3.2 continued

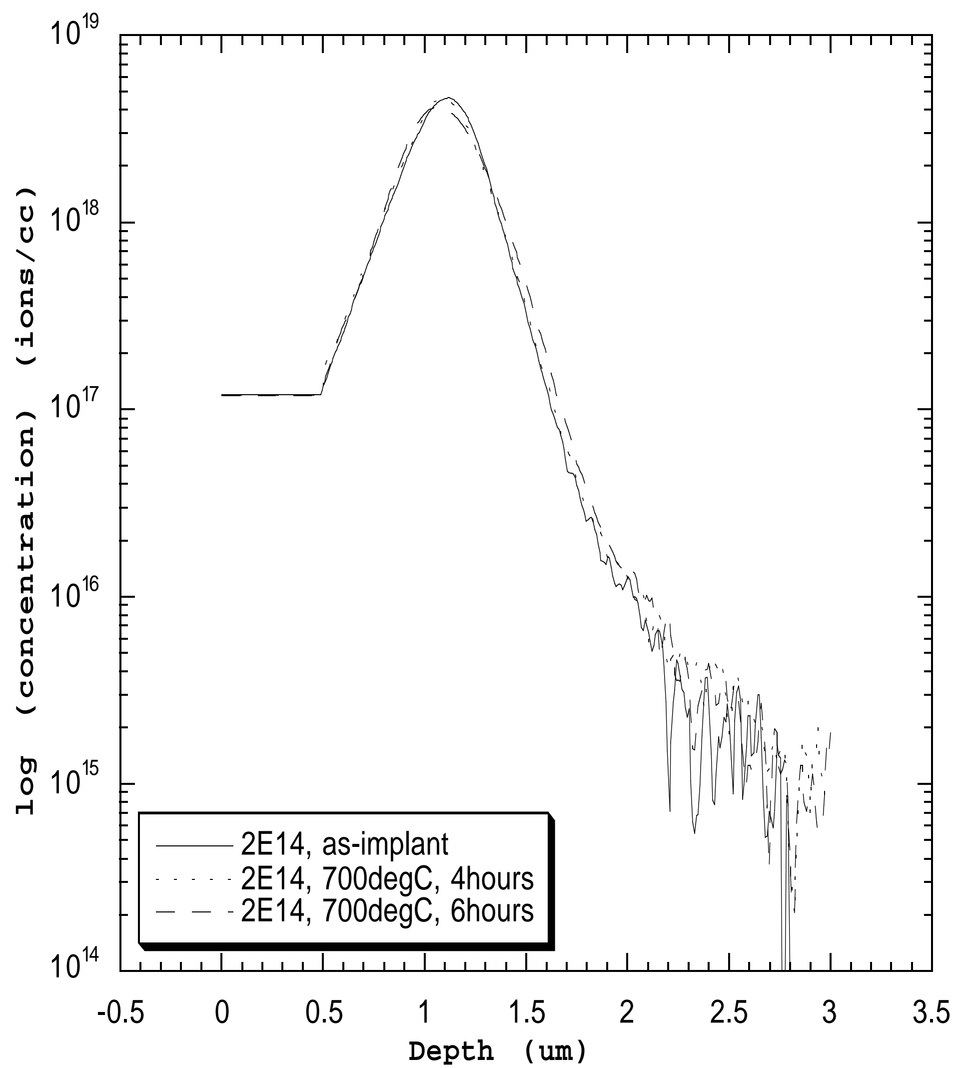

(i)

Figure 3.2 continued

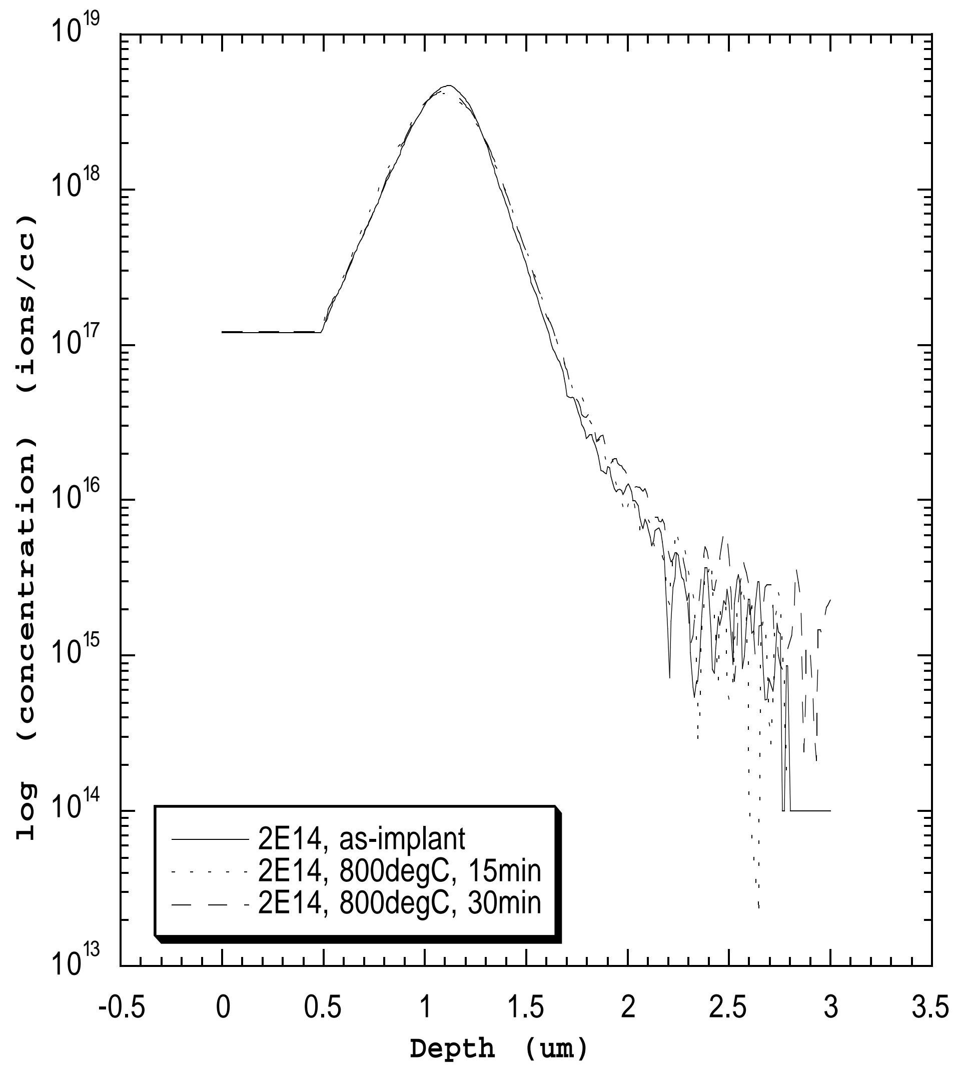

(j)

Figure 3.2 continued

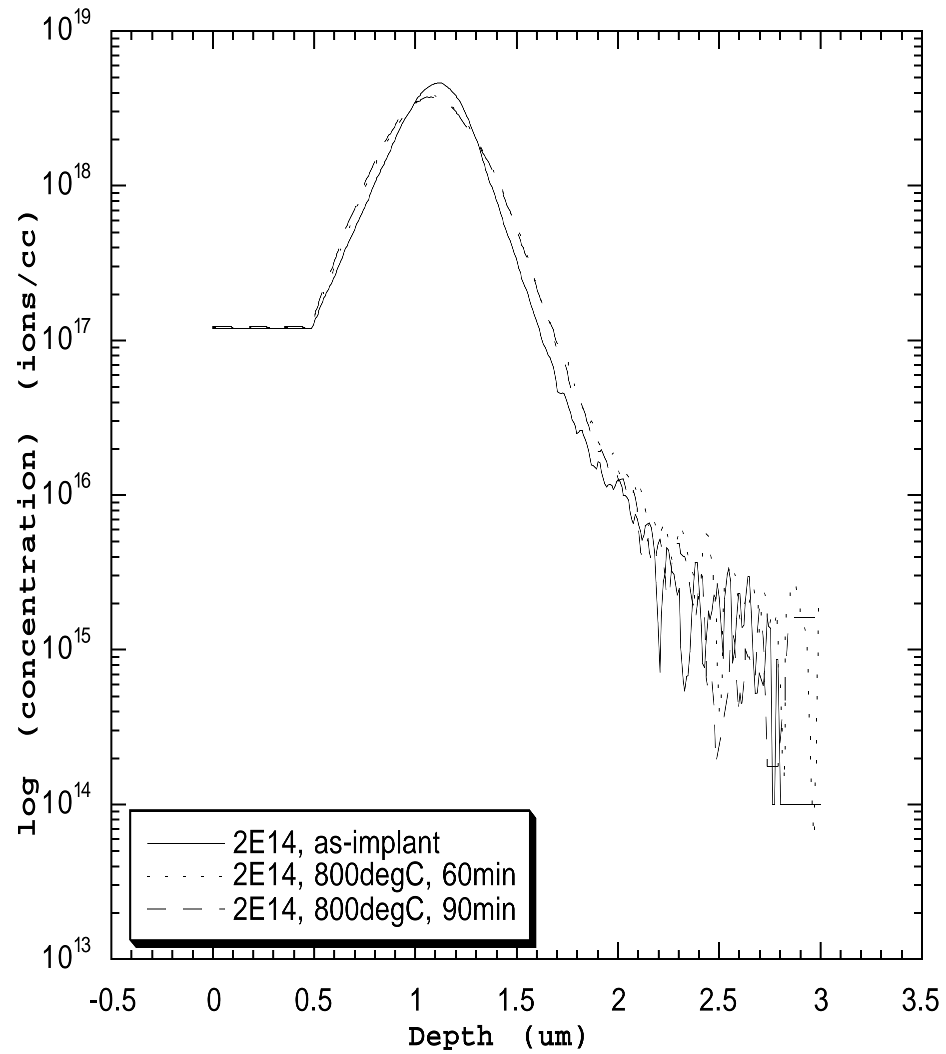

(k)

Figure 3.2 continued

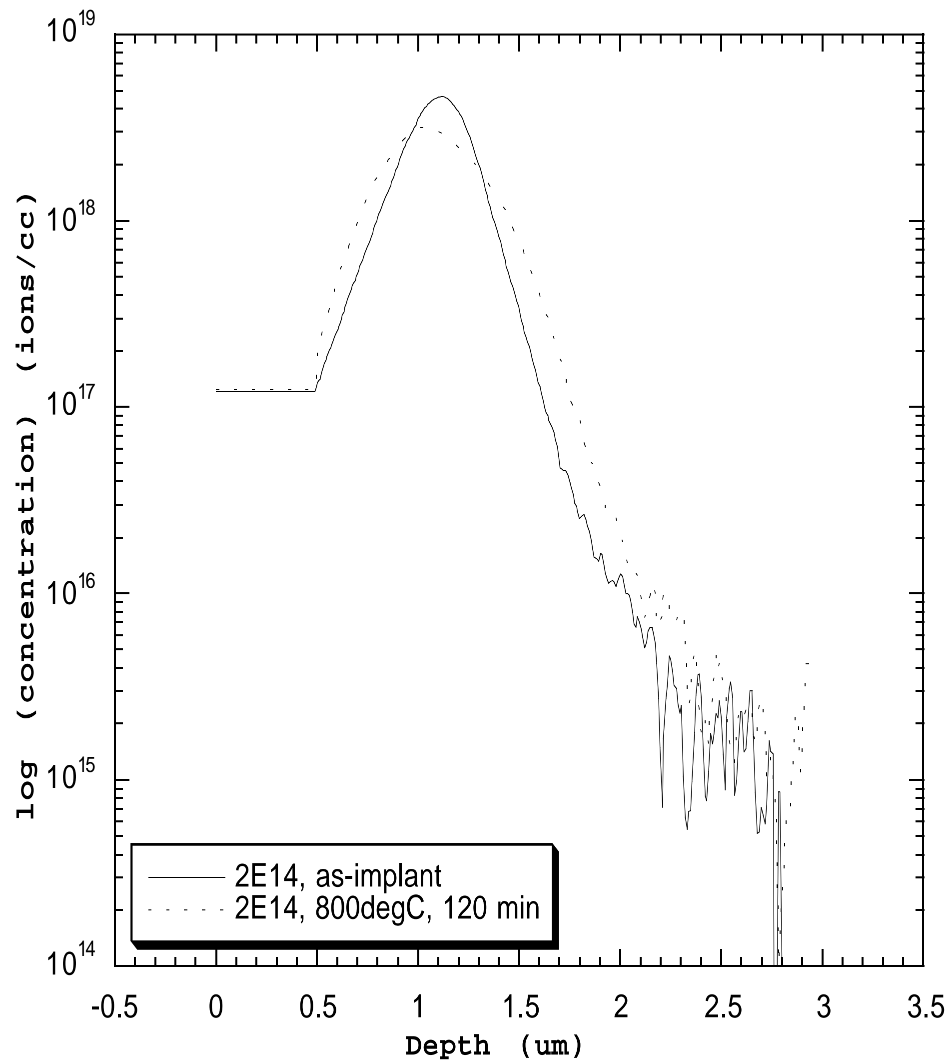

(l)

Figure 3.2 continued

Paul Packan[61] and other sources in the literature[55-57] have studied transient enhanced diffusion resulting from sub 200 KeV implants quite extensively. But these results cannot be extrapolated into the high energy regime without further investigation. This is because different damage structures might be affecting the transient diffusion at these high energy ranges.

3.3.1 Fitting to Experimental Profiles

The experimental set-up was as described in Section 3.2. The experimental (SIMS) profiles were fit with the simulated profiles to extract the diffusivity. Figure 3.3 shows the fits for one of the samples - this particular case being for 700°C, 5 * 10^{13}, 20 minutes anneal time. As can be seen in this figure, the X-axis is in microns and the Y- axis is the concentration on a logarithmic scale with units of ions/cc. With reference to Figure 3.3, the profile with a continuous line is the experimental (SIMS) profile. The profile as an alternately dashed line is the fit for the front (closer to the surface than R_p) of the profile. The profile with a regular dashed line is the fit for the back (farther away from the profile than R_p) of the profile. From Figure 3.3, it is clear that while the profile fit for the front, fits the front of the profile very well, it

does not fit well for the back of the profile. The converse is true for the profile fit for the back of the experimental profile. For example, the fit for the front is off by around 1500 angstroms at the back. This means that there is a difference in the diffusivity between the front and the back of the profile.

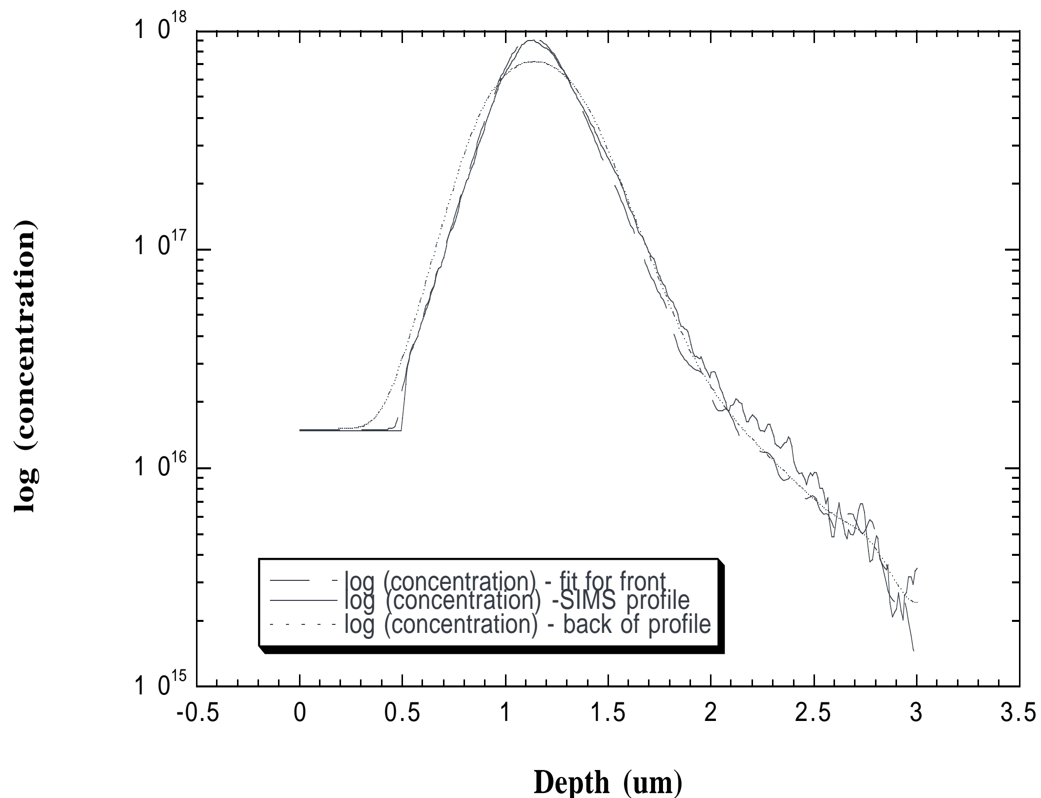

Figure 3.3: Fit for the front and back side of the profile for 5E13, 700°C, 20 minutes

From Figures 3.2 (a) - (l) we see that the profile depths are very deep--around 2 microns. In shallow implant profiles, the depths are in the range of only a

few thousands of angstroms. One may suspect that the differential enhancement as mentioned above might be a SIMS artifact due to roughening beyond the normal range (around 50 angstroms) as associated with SIMS experiments. Even if there was sufficient SIMS roughening, the as-implanted profiles and the experimental profiles should have the same error. This would tend to cancel when the diffusivity enhancement (D/D^*) value is extracted. It was also observed that the as-implanted profiles were the shallowest in depth and that the profiles increased in depth consistently with time. This consistency would not be expected if the observations were a SIMS error.

We also note from figures 3.4 - 3.7, that there is a shift in the range of the profile. This is due to an error in the SIMS measurement. The percent variation of the range is a maximum of 5% in the 5E13 samples and around 0.5% in the 2E14 samples. We note that while the shift in the range is negligible for the 2E14 samples, it is quite significant for the 5E13 samples. Hence range normalization was done for the 5E13 samples only.

Further, the SIMS technician who performed the SIMS also concurred that though the SIMS roughening could be greater than 50 angstroms due to the depths of the profiles involved, it still would not be on the order of a 1500 angstroms.

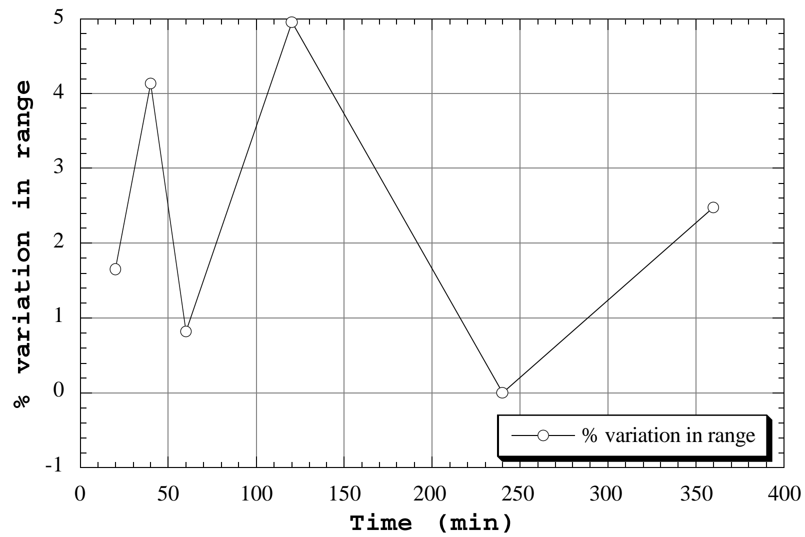

Figure 3.4: Range of the profiles of the 5E13, 700°C samples. The average range was 1.21 microns

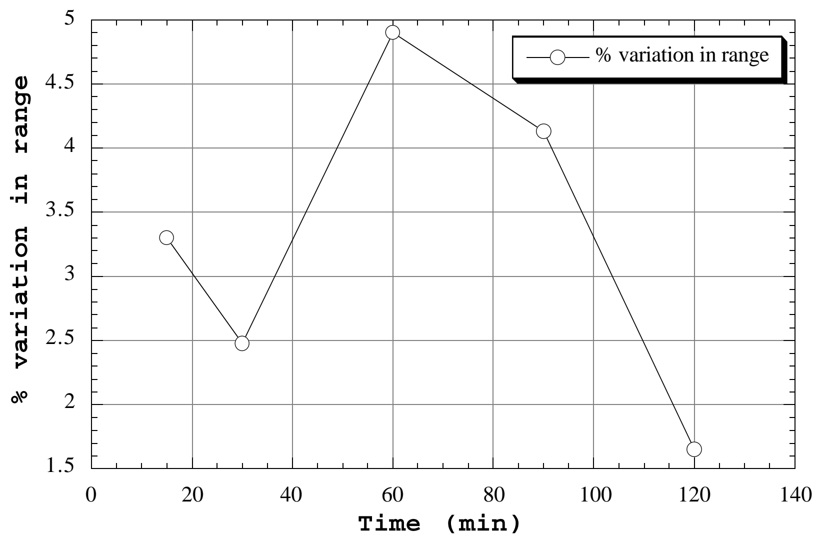

Figure 3.5: Range of the profiles of the 5E13, 800°C samples. The average range was 1.21 microns

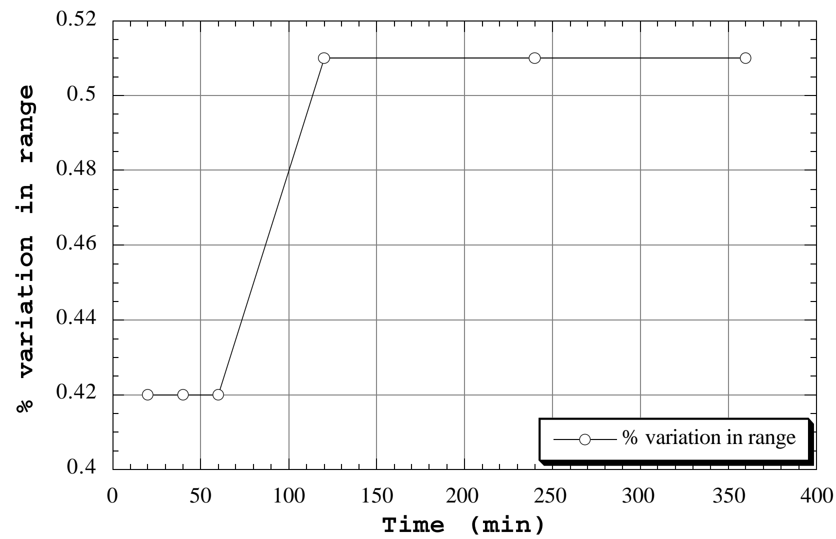

Figure 3.6: Range of the profiles of the 2E14, 700°C samples. The average range was 1.065 microns.

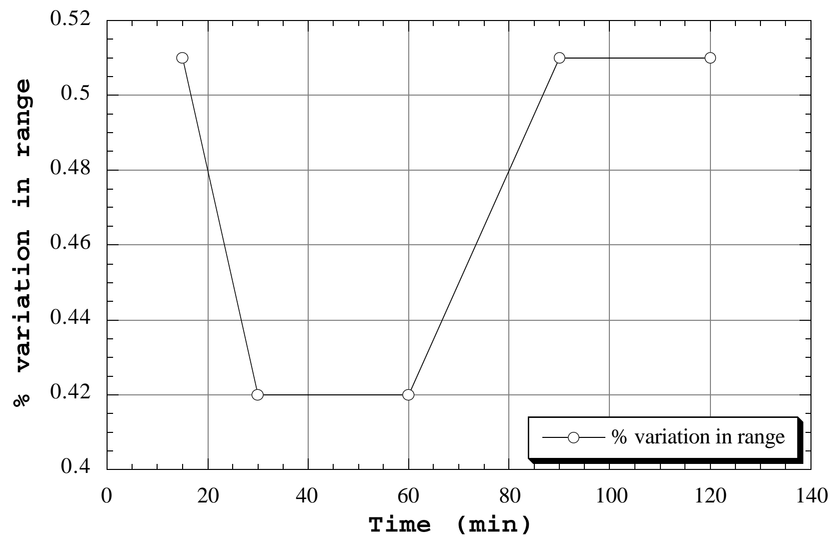

Figure 3.7: Range of the profiles of the 2E14, 800°C samples. The averange range was 1.065 microns

3.3.2 Diffusivity Enhancement (D/D^*) Plots

Figures 3.8 - 3.11 show the diffusivity enhancement at the various doses and temperatures used in this study. Since there is differential enhancement between the front and the back there are two (2) curves - one for the front of the profile and another for the back of the profile as marked . The detectability limit was also plotted assuming that the minimum observable motion of the profile was 100 angstroms. From these curves, we observe that the enhancement in diffusivity is more pronounced at the back of the profile than it is at the front. We also note that the differential enhancement is greater than the error bars. Hence, there is a differential enhancement taking place.

With reference to Figure 3.10, we note that there is almost no diffusivity enhancement except at 20 minutes and at 6 hours. The extent of differential diffusivity is not as pronounced in Figure 3.11.

The saturation times are expected to follow an $\exp(-t/\tau)$ characteristic as reported elsewhere in the literature[31]. Figure 3.8 shows such a characteristic. In this figure, the diffusivity enhancement of the front is below the detectability level for most of the time range of the experiment. In the plots of Figures 3.9, during the time range of the experiment, the decay in diffusivity enhancement is about a factor of 4 at the

back and a factor of 5 at the front. The decay is not as steep as what one would expect from low energy studies. Packan[61] has reported a saturation time of 45 minutes at 800°C for a comparable dose. Figure 3.11 shows that the enhancement is almost flat over the time range of the experiment.

The above discusion is an interesting observation compared to the low energy cases because this shows that the saturation times are much longer than expected for low energies. The examination of the plots of Figures 3.8 - 3.11, show that within the time range of the experiments, the saturation times are very far off from the times for which the experiments were done. The times for the experiments were set up based on a knowledge of the saturation times for the low energy (sub 200keV) cases. Since the experimental times are much shorter than the saturation times as argued above, it is not possible to say from the plots of Figures 3.8-3.11, if there is a difference in the saturation times between the front and the back of the profile.

The inert diffusivities used in the error calculation and the fits were the default values in FLOOPS. They are as follows:

$D^*(700^\circ C) = 8*10^{-19}\ cm^2/sec$

$D^*(800^\circ C) = 3.8*10^{-17}\ cm^2/sec$

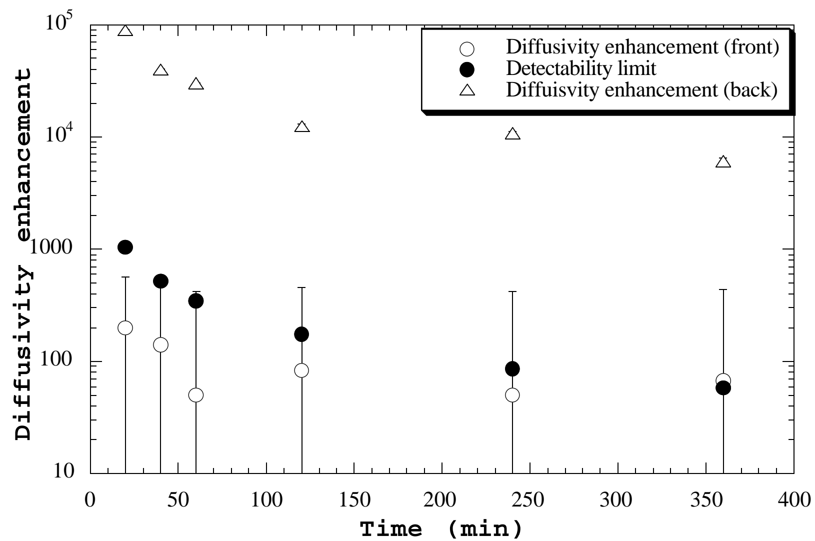

Figure 3.8: Diffusivity enhancement on semi logarithmic scale for 5E13, 700°C.

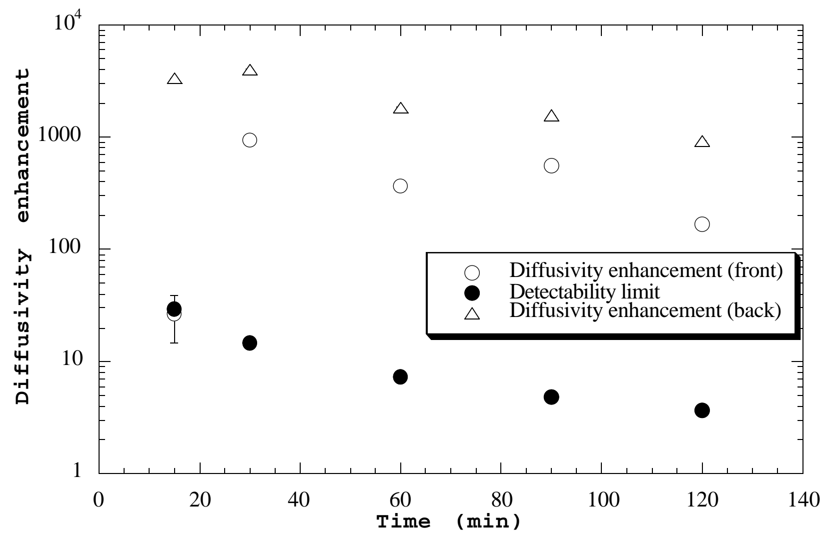

Figure 3.9: Diffusivity enhancement on semi logarithmic scale for 5E13, 800°C.

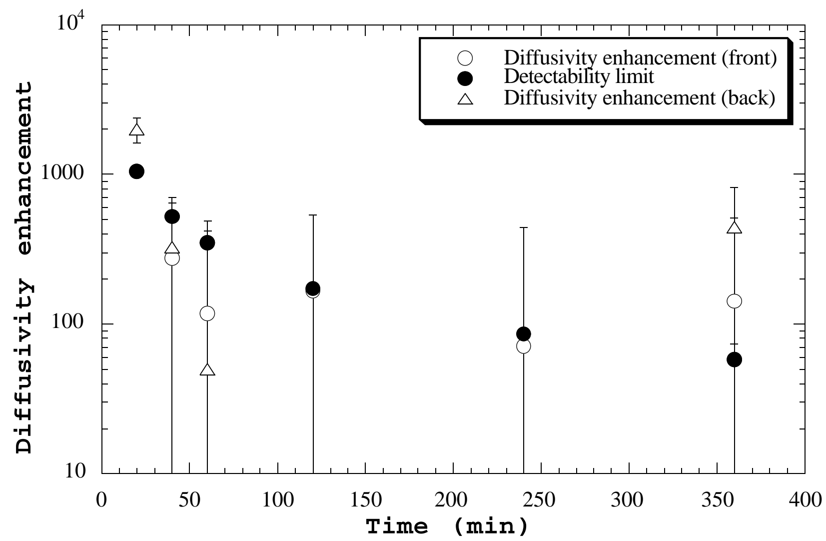

Figure 3.10: Diffusivity enhancement on semi logarithmic scale for 2E14, 700°C.

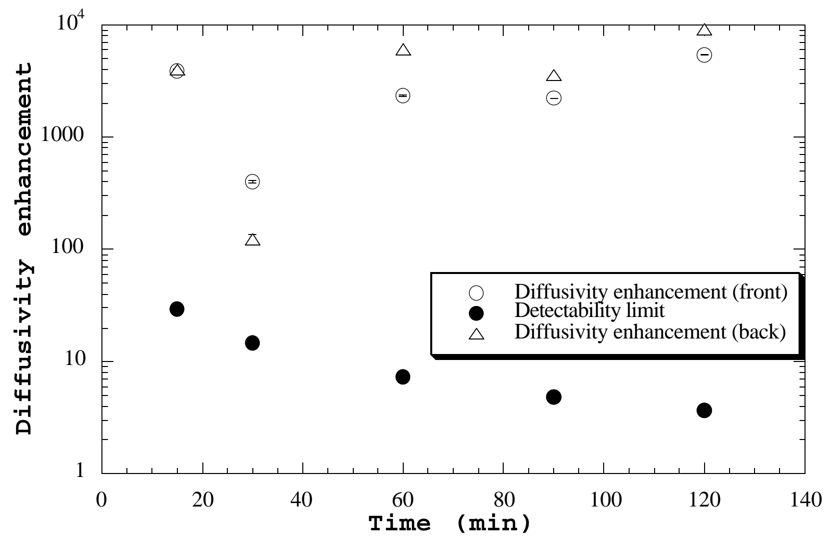

Figure 3.11: Diffusivity enhancement on semi logarithmic scale for 2E14, 800°C.

3.4 Discussion

From examining the above figures, it can be seen that there is a difference in motion of the diffusion front between the plots for the various combinations of the doses and temperatures used in this study. For example, on an examination of Figure 3.8, it is quite clear that there is a motion more than an order of magnitude at the back of the profile than that at the front of the profile even for short times. With reference to Figure 3.11, within the times for which the anneals were done, the diffusion front is almost flat indicating that the experimental times were well below the saturation times.

Further, we also note that the amount of transient diffusion is around 10 percent in relation to the total junction depth. This is evident from Figure 3.3. Here for example, the fit for the front is off by around 1500 to 2000 angstroms which accounts for around 10% of the junction depth.

In this study we note that there is differential enhancement and that the decay times are much longer than the low energy cases. A speculation of the mechanism is proposed here. One of the reasons for the differential enhancement could be that there is a vacancy supersaturation at the surface while there is only an equilibrium concentration of vacancies with a

supersaturation of interstitials in the bulk as pointed out by Servidori, *et.al*[47]. This would mean that due to vacancy supersaturation at the surface, the interstitials introduced due to implantation damage in this region would annihilate much more than those at the bulk where a much lesser concentration of vacancies is present. This argument would then imply a differential diffusivity enhancement.

Another explanation for the differential enhancement could be that bulk recombination alone is not enough to support the annihilation of interstitials. Because, had bulk recombination alone been responsible, one could argue that we should not have seen differential enhancement of diffusivity. But, clearly, this is not the case. So, though we create an excess of interstitials, we do not have enough vacancies to annihilate the excess interstitials. Hence the surface could play a role in the annihilation of the excess interstitials. Due to the depth of the profiles involved, there is a finite amount of time needed for the excess interstitials to reach the surface and be annihilated leading to longer saturation times. Infact, if this were the case, one can speculate that those interstitials before the implant peak, reach the surface quicker and hence have shorter decay times, while those beyond the peak take a longer time to reach the surface and have longer decay times. Of course, from the plots

of Figures 3.8 - 3.11, this is not evident as the saturation times are much larger than the times for which the experiment was performed.

There is also a possibility that secondary defects are formed and these influence the diffusion in some way. Shreutelkamp, *et. al.,*[62] have argued that the secondary defect formation depends critically on the number of silicon atoms ejected from their lattice positions and not on the dose. They suggest a value of $(5-6)*10^{16}$ displaced silicon atoms/cm^2 for the formation of secondary defects in Phosphorus doped wafers after annealing at $900^{o}C$ for 15 minutes. This translates into a dose of less than $5*10^{13}$ Phosphorus ions/cm^2 at an energy of 1MeV. So, even at the lowest dose of the experiment, there may be some secondary defects formed, at least at the higher time regimes. These defects may influence the diffusion coefficient enhancement values. But a point of caution here is that what is suggested is speculative at this point and needs further investigation.

CHAPTER 4
CONCLUSIONS

From the preceding discussion it is clear that there is a differential diffusivity between the front and the back of the profile and that the diffusivity enhancement is more at the back that it is at the front. Considerable differential diffusivity enhancement has been observed even at short times. While the extent of additional profile motion is around a 1500 angstroms and this might not be significant from a circuit or a device point of view, still, this study is significant from a physical viewpoint since it leads to a better understanding of transient diffusion. It also leads to a better understanding of the energy dependence of transient diffusion which was the goal of this study.

Further, the decay times are also much longer compared to the low energy implant cases. This is interesting, because the anneal times for the experiments were set up based on the saturation times required for anneals at low energy implants at comparable doses and temperatures. But we observed that the saturation times were much longer than those for the low energy implants.

These observations lead to some interesting speculations of the mechanism as described in Chapter 3.4. The enhancement of diffusivity was found to be greater at the back of the profile than at the front of the profile. Further, the saturation times were also larger than those of the low energy implant cases. As stated in Chapter 3, in Section 3.4, these observations indicate that there could be a vacancy supersaturation at the surface leading to differential enhancement of diffusivity or that the surface could act as a recombination site leading to enhanced diffusion until the interstitials are able to reach the surface and be annihilated eventually returning to their equilibrium concentration. This could explain the longer saturation times observed. The above mentioned observations could also be due to some extended defects being formed near the peak of the damage region and these could alter the diffusion kinetics in some way at the doses and anneal temperatures at which this study was done.

Further work based on this thesis could be to do a cross-sectional transmission electron microscopy (XTEM) analysis of the annealed wafers and investigate the mechanism based on the defects formed.

The other possible continuation of this work could be to see how the enhancement values scale with energy for a given species. Paul Packan[61], for example, has plotted diffusion enhancement vs. energy upto 200KeV for

^{29}Si implants onto Si. A similar plot could be done for Phosphorus over a magnitude range in energy, say from 100KeV to 1MeV. Also, one could go over the energy range over a magnitude, say from 100KeV to 1MeV and note when the differential enhancements start to occur and become "real" i.e. beyond the experimental error range of the experiment. Also to gain absolute confidence in the values presented, the experiment could be repeated for a higher energy dose, say 3MeV, and see if the same effects are observed and if there are any differences, then investigate as to why they are so. Also, the SIMS could be performed by changing a few of the SIMS analysis conditions. Of course, the trade-off here is cost. It has to be borne in mind that to perform SIMS it costs around $350/hour and hence repeating the SIMS experiment at additional conditions is proportionately going to scale-up the cost of the experiment.

Further, these effects could also be modeled in process simulators like FLOOPS and maybe even make it as a package where all the user needs to do is just type in the dose, energy, species, temperatures and anneal time and the enhanced diffusivity values pop up. If the user exceeds a energy and dose range, where differential enhancement starts to occur, then the differential enhancement values also should be generated. But, of course, this development cannot be made possible before the mechanism by which these effects occur and at what

energy and dose ranges these effects occur are investigated.

REFERENCE LIST

1. S. Wolf and R.N.Tauber, "*Silicon Processing for the VLSI Era*" Vol.1-Process Technology, Lattice Press, California 1990, 243 - 244

2. S.M.Hu, *Mat. Sci. and Engg. Reports*, **R13,** Nos.3-4, 1994

3. A.Seeger and K.P. Chik, *Phys. Stat. Solidi*, **29**, 455

4. P.G. Shewmon, *Diffusion in Solids,* McGraw-Hill, New York, 1963

5. R.B.Fair, "Concentration Profiles of diffused dopants in Silicon", in F.F.Y. Wang, Ed., *Impurity Doping Processes in Silicon,* North-holland, New York, 1981, Chapter 7

6. T.Y. Tan, U. Gosele and F. Morehead, *J. Applied Physics,* **A31**, 97 (1983)

7. T.Y. Tan and V.Gosele, *Proc. of VLSI Science and Technol.,* 1984, Vol. **84-7,** 151 (1984)

8. S.M. Hu, *J.Appl. Phys.,* **45**, 1567 (1974)

9. G.N.Will, *Solid State Electron.,* **12**, 133 (1969)

10. K.E.Beand and P.S. Gleim, *Proc. IEEE,* **57**, 1469 (1969)

11. T.C. Chan and C.C. Mai, *Proc. IEEE,* **58**, 588 (1970)

12. R.A. Kovalev, V.B.Bernikov, Yu I. Pashintev and V.A. Marasanov, *Sov. Phys. Solid State ,* **11**, 1571 (1970)

13. M.Okamura, *Jpn. J. Appl. Phys.,***9**, 849 (1970)

14. L.E. Katz, in *Silicon Device Processing,* Natl. Bur. Standards. Spec. Publ. 337, Washington DC, 1970, p.192

15. W.G.Allen and K.W.Anand, *Solid State Electron.,* **14**, 397(1971)

16. H.Higuchi, M.Maki and T.Takano, Electrochem. Soc. Meeting, Washington DC, Extended Abstract No. 78.

17. D.J.D. Thomas, *Phys. Stat. Solidi,* **3**, 2261 (1963)

18. H.J. Queisser and P.G.G. Van Loon, *J. Appl. Phys.,* **35**, 3066 (1964)

19. R.J. Jaccodine and C.M. Drum, *Appl. Phys. Lett.,* **8**, 29 (1966)

20. G.R. Brooker and W.J. Tunstall, *Phil. Mag.,* **13**, 71 (1966)

21. W.A. Fisher and J.A. Amick, *J. Electrochem. Soc.,* **113**, 1054 (1966)

22. P.B. Hirsch, A. Howie, R.B.Nicholson and D.W. Pashley, *Electon Microscopy of Thin Crystals,* Butterworths, London, 234 (1965)

23. H. Hashimoto, A. Howie and M.J. Whelan, *Proc. Roy. Soc.A,* **269**, 80 (1962)

24. S.M. Hu, *J. Appl. Phys.,* **51**, 3666 (1980)

25. W.B. Rogers and H.Z. Massoud, *J. Electrochem. Soc.,* **138**, 3492 (1991)

26. S. Mizuo and H. Higuchi, *Jpn. J. Appl. Phys.,* **20**, 739, (1981)

27. D.A. Antoniadis and I. Moskowtiz, *J. Appl. Phys.,* **53**, 6788 (1982)

28. S. Mizuo and H. Higuchi, *Jpn. J. Appl. Phys.,* **21**, 281, (1982)

29. Y. Hayafuji, K. Kajiwara and S. Usui, *J. Appl. Phys.,* **53**, 8639 (1982)

30. P. Fahey, R.W. Dutton and M. Moslehi, *Appl. Phys. Lett.,* **43**, 683 (1983)

31. S. Mizuo, T. Kusaka, S. Shintani, M. Nanba and H. Higuchi, *J. Appl. Phys.,* **54**, 3860 (1983)

32. P. Fahey, G. Barbuscia, M. Moslehi and R.W. Dutton, *Appl. Phys. Lett.,* **46**, 784 (1985)

33. H. Strunk, U. Gosele and B.O. Kobbesen, *Appl. Phys. Lett.,* **34**, 530 (1979)

34. P. Fahey, R.W. Dutton, S.M. Hu, *Appl. Phys. Lett.,* **44**, 777 (1984)

35. U. Gosele, W. Frank, A. Seeger, *Appl. Phys Lett.* **23,** 361 (1980)

36. Gary B. Bronner, James D. Plummer, *J. Appl. Phys.* **61**, 5286 (1987)

37. H. Zimmerman, H. Ryssel, *Appl. Phys A*, **55**, 121 (1992)

38. H. Zimmerman, H. Ryssel, *J. Electrochem. Soc.,* **139**, No.1, 256 (1992)

39. S. Coffa, G. Franco, C.M. Camalleri, A. Giraffa, *J. Appl. Phys.,* **80**, 161 (1996)

40. R.T. Hodgson, V.R. Deline, S. Mader, J.C. Gelpey, *Appl. Phys. Lett.,* **44,** 589 (1984)

41. L.C. Hopkins, T.E. Seidel, E. Landi, S. Solmi, *J.Electrochem. Soc.,* **32,** 2035 (1985)

42. K. Cho, M. Numan, T.G. Finstad, W.K. Chu, J. Liu, J.J. Wortman, *Appl. Phys. Lett.,***47**, 1321 (1985)

43. S.J. Pennycook, J. Narayan, O.W. Holland, *J.Elecrochem. Soc.,* **132**, 1962 (1985)

44. R. Angelucci, P. Negrini, S. Solmi, *Appl. Phys. Lett.,* **49,** 1468 (1986)

45. N.E.B. Cowern, D.J. Godfrey, D.E. Sykes, *Appl. Phys. Lett.,* **49**, 1711 (1986)

46. M. Servidori, Z. Sourek, S. Solmi, *J. Appl. Phys.,* **62**, 1723 (1987)

47. M. Servidori, R. Angelucci, F. Cembali, P. Negrini, S. Solmi, *J.Appl. Phys.,* **61,** 1834 (1987)

48. A.E. Michael, W. Rausch, P.A. Roseheim, R.H. Kastl, *Appl. Phys. Lett.,* **50**, 416 (1987)

49. A.E. Michael, W. Rausch, P.A. Roseheim, *Appl. Phys. Lett.,* **51**, 487 (1987)

50. M. Miyake, S. Aoyama, *J.Appl. Phys.,* **63**, 1754 (1988)

51. T.O. Sedgwick, A.E. Michael, V.R. Deline, S.A. Cohen, J.B. Lasky, *J.Appl. Phys.,* **63**, 1452 (1988)

52. S. Solmi, F. Cembali, R. Fabbri, M. Servidori, R. Canteri, *Appl. Phys. Lett.,* **48**, 255 (1989)

53. M. Servidori, S. Solmi, P.Zaumseil, U. Winter, M. Anderle, *J.Appl. Phys.,* **65**, 98 (1989)

54. Q. Guo, X. Bao, J. Hong, Y. Yan, D. Feng, *Appl. Phys. Lett.,* **54**, 1433 (1989)

55. P.A. Packan, J.D. Plummer, *Appl. Phys.Lett.,* **56**, 1787 (1990)

56. Martin D., *J. Electrochem. Soc.,* **138**, No. 4, 1160 (1991)

57. D.J. Eagelsham, P.A.Stolk, H.J.Gossman and J.M.Poate, *Appl. Phys. Lett.,* **65**, 2305 (1994)

58. J.M. Poate, D.J.Eagelsham, G.H.Gilmer, H.Gossmann, M.Jaraiz, C.S.Rafferty and P.A.Stolk*, IEDM***,** 77 (1995)

59. J.Y. Cheng, D.J.Eaglesham, D.C.Jacobson, P.A.Stolk, J.L. Benton, J.M.Poate, *J.Appl. Phys.,* **80**, 2105 (1996)

60. C.S. Rafferty, H.J. Gossmann, A. Kamgar, D.C. Jacobson, E.J. Lloyd, S.J. Hillenius, H.H. Vuong, J. Becerro, H.M. Vaidya, S.A. Lytle, M.J. Thoma, H.S. Luftman, *IEDM*, 791 (1996)

61. P.A. Packan, PhD. Thesis, Stanford University, 1991

62. Schreutelkamp, Liefting, *et. al.,* Mat. Sci. Reports, **6**, 275 (1991)

BIOGRAPHICAL SKETCH

Lahir S. Adam was born at Madras, India in April 1972. He did his schooling at San Thome Higher Secondary School, Mylapore, Madras, India. He graduated with a B.S. in electrical engineering with distinction from the Regional Engineering College, Trichy, India in May of 1993. He worked as a Process Engineer with the Complementary Metal Oxide Semiconductor (CMOS) group for the Department of Defense, India for the period September 1993 - July 1995. He started his graduate education at the University of Florida in the Fall of 1995. His professional interests are in the area of diffusion and implantation. After completing his Master of Science degree at the University of Florida, he plans to pursue a PhD in the same field.